

Journal Pre-proof



Unfermented β -fructan fibers fuel inflammation in select inflammatory bowel disease patients

Heather K. Armstrong, Michael Bording-Jorgensen, Deanna M. Santer, Zhengxiao Zhang, Rosica Valcheva, Aja M. Rieger, Justin Sung-Ho Kim, Stephanie I. Dijk, Ramsha Mahmood, Olamide Ogungbola, Juan Jovel, France Moreau, Hayley Gorman, Robyn Dickner, Jeremy Jerasi, Inderdeep K. Mander, Dawson Lafleur, Christopher Cheng, Alexandra Petrova, Terri-Lyn Jeanson, Andrew Mason, Consolato M. Sergi, Arie Levine, Kris Chadee, David Armstrong, Sarah Rauscher, Charles N. Bernstein, Matthew W. Carroll, Hien Q. Huynh, Jens Walter, Karen L. Madsen, Levinus A. Dieleman, Eytan Wine

PII: S0016-5085(22)01150-7
DOI: <https://doi.org/10.1053/j.gastro.2022.09.034>
Reference: YGAST 65355

To appear in: *Gastroenterology*
Accepted Date: 23 September 2022

Please cite this article as: Armstrong HK, Bording-Jorgensen M, Santer DM, Zhang Z, Valcheva R, Rieger AM, Sung-Ho Kim J, Dijk SI, Mahmood R, Ogungbola O, Jovel J, Moreau F, Gorman H, Dickner R, Jerasi J, Mander IK, Lafleur D, Cheng C, Petrova A, Jeanson T-L, Mason A, Sergi CM, Levine A, Chadee K, Armstrong D, Rauscher S, Bernstein CN, Carroll MW, Huynh HQ, Walter J, Madsen KL, Dieleman LA, Wine E, Unfermented β -fructan fibers fuel inflammation in select inflammatory bowel disease patients, *Gastroenterology* (2022), doi: <https://doi.org/10.1053/j.gastro.2022.09.034>.

This is a PDF file of an article that has undergone enhancements after acceptance, such as the addition of a cover page and metadata, and formatting for readability, but it is not yet the definitive version of record. This version will undergo additional copyediting, typesetting and review before it is published in its final form, but we are providing this version to give early visibility of the article. Please note that, during the production process, errors may be discovered which could affect the content, and all legal disclaimers that apply to the journal pertain.

© 2022 by the AGA Institute

Unfermented β -fructan fibers fuel inflammation in select inflammatory bowel disease patients

Short Title: Dietary fibers promote inflammation in IBD

Heather K. Armstrong^{1,2,3*}, Michael Bording-Jorgensen^{1,2}, Deanna M. Santer⁴, Zhengxiao Zhang^{1,5,6}, Rosica Valcheva^{1,5}, Aja M. Rieger⁷, Justin Sung-Ho Kim^{8,9}, Stephanie I. Dijk^{1,10}, Ramsha Mahmood³, Olamide Ogungbola⁴, Juan Jovel¹, France Moreau¹¹, Hayley Gorman¹¹, Robyn Dickner^{1,2}, Jeremy Jerasi^{1,2}, Inderdeep K. Mander^{1,2}, Dawson Lafleur^{1,2}, Christopher Cheng^{1,2}, Alexandra Petrova², Terri-Lyn Jeanson³, Andrew Mason^{1,5}, Consolato M. Sergi¹², Arie Levine¹³, Kris Chadee¹¹, David Armstrong⁸, Sarah Rauscher^{8,9,14}, Charles N. Bernstein³, Matthew W. Carroll², Hien Q. Huynh², Jens Walter^{1,15}, Karen L. Madsen^{1,5}, Levinus A. Dieleman^{1,5}, Eytan Wine^{1,2,10*}

¹ Centre of Excellence for Gastrointestinal Inflammation and Immunity Research, University of Alberta, Edmonton, AB, T6G 2X8, Canada

² Department of Pediatrics, University of Alberta, Edmonton, AB, T6G 1C9, Canada

³ Department of Internal Medicine, University of Manitoba, Winnipeg, MB, R3E 0W2, Canada

⁴ Department of Immunology, University of Manitoba, Winnipeg, MB, R3E 0T5, Canada

⁵ Department of Medicine, Division of Gastroenterology, University of Alberta, Edmonton, AB, T6G 2X8, Canada

⁶ College of Food and Biological Engineering, Jimei University, Xiamen, Fujian, 361000, China

⁷ Department of Medical Microbiology and Immunology, University of Alberta, Edmonton, AB, T6G 2G3, Canada

⁸ Department of Chemical and Physical Sciences, University of Toronto Mississauga, Mississauga, ON, L5L 1C6, Canada

⁹ Department of Physics, University of Toronto, Toronto, ON, M5S 1A7, Canada

¹⁰ Department of Physiology, University of Alberta, Edmonton, AB, T6G 2G3, Canada

¹¹ Department of Microbiology, Immunology and Infectious Disease, University of Calgary, Calgary, AB, T2N 4N1, Canada

¹² Anatomic Pathology Division, Children's Hospital of Eastern Ontario, Ottawa, ON, K1H 8L1 Canada

¹³ Pediatric Gastroenterology Unit, Wolfson Medical Center, Tel-Aviv University, Holon, 5822012, Israel

¹⁴ Department of Chemistry, University of Toronto, 80 St. George Street, Toronto, ON M5S 3H6, Canada

¹⁵ APC Microbiome Ireland, School of Microbiology, and Department of Medicine, University College Cork, Cork, T12 YT20, Ireland

*Correspondence:

Dr Heather Armstrong; Department of Internal Medicine, University of Manitoba, 808 JBRC, 715 McDermot Ave, Winnipeg, MB, Canada; Heather.Armstrong@umanitoba.ca,

Dr Eytan Wine; Department of Pediatrics, University of Alberta, 7-124 Katz Building, 114st and 87ave, Edmonton, AB, T6G 1C9, Canada; wine@ualberta.ca

Grant support: The funders had no role in study design, collection, or interpretation of data. The following grants were used to fund the project: Weston Family Foundation Microbiome Initiative grant (EW, HA, RV, LD). Natural Sciences and Engineering Research Council (NSERC) and Manitoba Medical Services Foundation (MMSF) grants (HA). Canadian Institute of Health Research grant (EW). Canadian Institute of Health Research postdoctoral fellowship (HA). International Society for the Advancement of Cytometry Shared Resource Lab Emerging Leader (AR).

Abbreviations: NF no fiber; FOS oligofructose; SCFA short chain fatty acid; FFQ food frequency questionnaire.

Disclosures: Authors declare that they have no competing interests.

Author contributions: HKA and EW conceived, developed, and coordinated the project. HKA, AP, MWC, HQH, RV, CNB, TJ, LAD and EW acquired the patient consent, and collected and processed mucosal washings and biopsy tissues. LAD provided the samples from the RCT intervention in adult UC patients. HKA, RV, DMS, MB-J, AMR, RD, JJ, IM, FR, HG, ZZ, JJ, JK, RM, OO, CC and DL performed and/or analyzed experiments. HKA, AMR, ZZ, SD, and HG were responsible for the figure preparation and statistical analyses. CMS provided unbiased histological confirmation. MC, HH, AM, KC, JW, KM, AL, SR, DA and LAD provided additional supervision and oversight. HKA drafted the manuscript. All authors contributed to manuscript edits and approved the final version of the manuscript.

Data Transparency Statement: Study data, analytic methods, and materials have been made available to other researchers in the main text or the supplementary materials; there are no restrictions on data availability. Shotgun metagenomics raw sequencing reads were deposited at the Short Reads Archive (SRA) database of NCBI and are publicly available under accession number PRJNA690735.

Abstract

Background and aims: Inflammatory bowel diseases (IBD) are impacted by dietary factors, including non-digestible carbohydrates (fibers), which are fermented by colonic microbes. Fibers are overall beneficial but not all fibers are alike and some IBD patients report intolerance to fiber consumption. Given reproducible evidence of reduced fiber-fermenting microbes in IBD patients, we hypothesized that fibers remain intact in select patients with reduced fiber-fermenting microbes and can then bind host cell receptors, subsequently promoting gut inflammation.

Methods: Colonic biopsies cultured *ex vivo* and cell lines *in vitro* were incubated with oligofructose (5g/L), or fermentation supernatants (24hr anaerobic fermentation) and immune responses (cytokine secretion [ELISA/MSD] and expression [qPCR]) were assessed. Influence of microbiota in mediating host response was examined and taxonomic classification of microbiota was conducted with Kraken2 and metabolic profiling by HUMAnN2, using R software.

Results: Unfermented dietary β -fructan fibers induced pro-inflammatory cytokines in a subset of IBD intestinal biopsies cultured *ex vivo*, and immune cells (including peripheral blood mononuclear cells). Results were validated in an adult IBD randomized controlled trial examining β -fructan supplementation. The pro-inflammatory response to intact β -fructan required activation of the NLRP3 and TLR2 pathways. Fermentation of β -fructans by human gut whole-microbiota cultures reduced the pro-inflammatory response, but only when microbes were collected from non-IBD or inactive IBD patients. Fiber-induced immune responses correlated with microbe functions, luminal metabolites, and dietary fiber avoidance.

Conclusion: While fibers are typically beneficial in individuals with normal microbial fermentative potential, some dietary fibers have detrimental effects in select patients with active IBD who lack fermentative microbe activities.

Keywords

Dietary fibers, microbiome, IBD, fermentation

ACKNOWLEDGEMENTS

We graciously thank the patients and their families for agreeing to participate and provide data and samples, as well as the IBD research coordinators, nurses, and endoscopy staff at Stollery Children's Hospital in Edmonton and Health Sciences Centre in Winnipeg. We would like to acknowledge The Applied Genomic Core, Flow Cytometry Core, and Chromatography Core at the University of Alberta for their help in experiment preparations and technical procedures, along with Dr Chris Siow at the University of Manitoba St Boniface Hospital for technical support. We also thank CEGIR for providing material support.

Introduction

Digestible carbohydrates are degraded in the small intestine; non-digestible carbohydrates (fiber and resistant starch) are fermented by colonic microbes.¹ Fermentation of dietary fibers produces gases, lactate, and short chain fatty acids (SCFAs),^{2,3} with multiple beneficial physiological effects,³ but fibers have also been shown to be harmful in select situations.^{4,5} The beneficial potential for fermentable fibers in inflammatory bowel diseases (IBD) is demonstrated by low SCFA production, especially in ulcerative colitis (UC), linked to absence of SCFA-producing microbes.⁶ Administration of β -fructan fibers improved mild UC, associated with increased SCFA (butyrate) production.^{2,7} However, this generally positive effect of fibers related to fermentation and SCFA production seems to have overshadowed potential detriments, as many patients with IBD describe sensitivity to fiber consumption,⁸ ignoring or not understanding this process can lead to avoiding non-digestible fibers altogether through exclusion diets.⁹⁻¹¹ Such exclusion diets can improve symptoms but may deprive patients of the benefits of fibers, which are especially important in IBD.²

While research has intensified on the role of fiber fermentation in IBD, and β -fructan fibers in particular have been gaining attention for their prebiotic potential (promoting growth of 'beneficial microbes'),^{7,12} the role of microbiota and fiber fermentation processes, and whether they are beneficial or detrimental, remains poorly understood. Structurally, dietary fibers (**Table S1**) and cell wall components of microorganisms (*e.g.*, fungal β -(1,3)glucans) are polymers of greater than 3 sugars (oligofructose [FOS] ~8 sugars; grain β -D-glucan ~3 sugars) and ranging up to 50-100 sugars (inulin; fungal β -(1,3)glucan), which can vary in their degree of polymerization (DP), branching, solubility, and interactions with host cells. Immune response to polysaccharides on the surface of fungal cells suggests a possible link between whole unfermented fibers and inflammation.^{13,14} β -(1,3)glucan on the surface of fungi (*e.g.*, zymosan, curdlan) interacts with immune cells (*e.g.*, macrophages), inducing pro-inflammatory antifungal immunity via Dectin-1 and TLR2.^{13,14} Similarly, β -fructan fibers (inulin and FOS) induce TLR-mediated inflammatory pathways.^{15,16} This led us to hypothesize that in patients with reduced fiber-fermenting microbes (*e.g.*, IBD), dietary fibers could remain intact, interact with host cell receptors, and promote gut inflammation. Here we demonstrate that unfermented dietary β -fructans induce pro-inflammatory cytokine secretion in select IBD patients, mediated by microbial functions. Our data suggest that select fibers may be detrimental in individuals lacking fermentative microbes (*e.g.*, IBD, other chronic illnesses, antibiotic use), with increased opportunity for interactions between host immune cells and luminal contents (due to increased immune cells and disrupted epithelial barrier). These same fibers provide health benefits in individuals with high fermentative potential.

Materials and Methods

Complete methods are available in the supplementary materials.

Consent and ethics approval

Consent/assent was obtained from patients/guardians; approved by the University of Alberta Health Research Ethics Board (Study IDs Pro00023820 and Pro00092609), Edmonton, AB, Canada. Blood donors consented for isolation of

Armstrong *et al.* 2022

human cells (Study ID Pro00046564). The randomized control trial (RCT) protocol was approved by Ethics Board at the University of Alberta (Study ID Pro00041938) and Natural Health Directorate at Health Canada. The study is publicly accessible at the U.S. National Institute of Health database (clinicaltrials.gov identification number NCT02865707).

Patient criteria and sample collection

Patients aged 3–18 years, with histological and endoscopic confirmed Crohn disease (CD) or UC, or non-IBD controls undergoing colonoscopy for symptoms suspected to be IBD, confirmed as normal (**Table S1**). Patient sample collection scheme provided (**Figure S1**) are explained in depth in supplementary methods section.

Cell lines and reagents

Cultures were incubated (37°C, 5% CO₂) and maintained as described in supplementary methods. Cell lines included human THP-1 macrophage (supplementary methods) and T84 cells (DMEM/F12, 10% FBS, 100U/mL penicillin, 100ug/ml streptomycin sulfate). PBMCs were isolated from non-IBD individuals with Lymphoprep™ Density Gradient Medium (STEMCELL Technologies). All cultures were treated with 250µl of fibre or fructose (Sigma Aldrich) prepared in PBS and 5% culture media (**Table S2**). Inhibition studies utilized stimulation YVAD (50 uM), Glyburide (200 uM), MCC950 (1uM), or TL2-C29 (75 uM) for 1 hr.

Ex vivo culture of patient biopsy tissues

Biopsy tissues collected from non-inflamed regions during colonoscopy were dissected into 1-mm³ pieces and cultured in duplicate (supplementary methods) with 250µl fiber solution (PBS, fiber, 5% DMEM/F12 [5%FBS], 100U/mL penicillin/100µg/mL streptomycin) at 37°C for 24hrs. Supernatants were collected for ELISA and biopsies were transferred to lysing matrix D bead beat tubes (MPbio) with 500µl TRIzol and stored at -80C for RNA isolation.

ELISA

Supernatants were centrifuged at 14000g for 10min to remove debris. Secreted IL-1β was measured following manufacturers protocol (R&D Systems). Sample/standard were added in duplicate; absorbance was measured at 450nm with 540nm; correction calculated using GraphPad Prism. Alternatively, multiplex ELISA (Mesoscale Discovery) examined secretions from biopsies, PBMC, and cell cultures following manufacturers protocols.

Flow Cytometry

Biopsy tissues were prepared for flow cytometry as described in supplementary methods. Cells were acquired on an Attune NxT flow cytometer (BVRY configuration, ThermoFisher Scientific). Data analysis was completed using FlowJo V9 (BD Biosciences). Cells were gated based on FSC/SSC; single cells were gated on FSC-A/FSC-H; immune cells were gated for CD45. Cell populations were analyzed using cell type specific markers. All gate boundaries were set using FMO controls.

Fructose assay

Fructose concentration in unfermented fiber solutions was determined by fructose assay kit, following manufacturer's directions (Abcam). To account for glucose interference, a series of fiber control solutions were prepared without fructose converting enzyme.

RNA isolation and gene expression analysis

RNA extraction was performed by Direct-zol microRNA prep kit (Zymo Research). Libraries were prepared using Superscript IV VILO Mastermix (Thermo Fisher). *Ex vivo* biopsies and cell lines were analysed by human chemokines

Armstrong *et al.* 2022

RT-qPCR arrays (Origene, and Qiagen) and validated by RT-qPCR using indicated genes (**Table S3**) and were analysed using CFX Manager Software V3.0 (Bio-Rad Laboratories, Inc.).

Trans-Epithelial Electrical Resistance (TEER)

T84 cells were seeded on the apical side of a 12mm, 0.4µm Transwells (Corning). Fibres were added to the apical wells and TEER was measured daily using a Millicell ERS voltohmmeter together with a STX1 electrode from World Precision Instruments (WPI). The fiber containing media was replaced every two days.

Molecular Docking of β-fructan (represented by Kestose-1) to TLR2 Heterodimers

We used two crystal structures containing TLR2 heterodimers for docking: TLR1-TLR2 (PDB ID: 2Z7X) and TLR2-TLR6 (PDB ID: 3A79). First, molecular dynamics (MD) simulations were carried out on these heterodimers. The simulations were used to provide an ensemble of conformations in solution to account for target flexibility.

Anaerobic culture of patient intestinal washes

Whole microbiota liquid cultures were obtained from patient intestinal washes, and immediately isolated and cultured anaerobically. Culture density was measured on a spectrophotometer then back-diluted to an OD₆₀₀ of 1.0 and split into two equal samples. Microbe pellets were collected and resuspended in 10mL NF or oligofructose (5mg/mL) solution, supplemented with 5% BHI for 24hr. Microbes were prepared for sequencing; supernatants were used as fermentation by-product solutions (SCFA gas chromatography) and pre-fermentation solution for incubation with THP-1 macrophage cells.

Gas chromatography for volatile fatty acids

SCFA concentrations were determined using volatile fatty acid (VFA) analysis by gas chromatography. Samples containing 5% phosphoric acid were combined with 200µL internal standard (isocaproic acid) in a GC vial and run on a 430-GC with FID (Varian, Inc., USA) using a Stabilwax-DA fused silica column (Restek Corp., 30m, 0.53mm ID, 0.5µm film), carrier gas helium 10ml/min, injector/detector temperatures maintained at 250°C, and injection split 5:1. The injection volume was 1µL. The oven was held for 0min at 80°C, then increased to 180°C at 20°C/min and held for 3min for a total run time of 8min, as determined using standard compounds and internal standard.

NGS library construction and shotgun metagenomics

Library construction and sequencing

Genomic DNA from aspirate washes was extracted using the QIAamp DNA Stool Mini Kit (Qiagen) with additional steps described in the supplementary methods. Libraries were constructed using Nextera XT DNA Preparation Kit (Illumina Inc.). Libraries were assayed on QIAxcel Fragment Analyzer System (Agilent) and quantified using Qubit Fluorometer. Multiplexed libraries were sequenced on a NovaSeq 6000 system (Illumina Inc.) using S2 flow cell at an average depth of 100 million reads per sample.

Bioinformatics analysis

Sequences were inspected with Fastqc and end read bases with quality scores <30 were trimmed with mcf-fastq allowing a 120 base pair minimal trimmed length. Taxonomic classification was conducted with Kraken2 and metabolic profiling by HUMAnN2 as described in supplementary methods.

Metabolomics

Armstrong *et al.* 2022

Metabolites were isolated from patient stool samples as directed by the Calgary Metabolomics Research Facility, University of Calgary.

Food frequency questionnaire

Food frequency questionnaire (FFQ), described in detail in supplementary methods, was considered valid if completed within 90 days of specimen collection. Estimated caloric values were generated using the Canadian Nutrient File database. Estimated daily kilocalorie values were calculated for each patient and verified against patient age and weight. A fiber content database (**Table S4**) was generated utilizing published data on food fiber contents, used to calculate approximate daily intakes of inulin, oligofructose, pectin, and β -glucan (kilocalorie-adjusted by Willett residuals method). Spearman correlation with fiber content was analyzed in Stata 14.

Quantification and Statistical Analysis

Shotgun metagenomics data analysis

Raw sequencing reads were deposited at the Short Reads Archive (SRA) NCBI database, publicly available under accession number PRJNA690735. Full data analysis methods are detailed in supplementary methods. Separate random forest classifiers (RFCs) were independently trained on changes in fecal microbial composition and enzymes and area under the receiver operating characteristic curves (AUC-ROCs) were used to evaluate RFC performance. Mann Whitney U test were performed between the response to oligofructose and its best predictors.

Statistical Analysis

In addition to specific statistical methods described, groups were compared using paired Wilcoxon *t*-test (two-tailed) analysis, ANOVA, or Kendall, depending on the relevant question, using GraphPad Prism. A *p*-value of <0.05 was considered significant in all cases and all error deviations are described by \pm SEM.

Results

β -fructans (inulin and FOS) induced inflammation in cell models and IBD

To assess if select intact fibers (**Table S1**) can stimulate a pro-inflammatory response, we utilized a human colonic tissue explant model (**Fig. S1**: outlines study design). To examine cell heterogeneity we first defined specific immune cell types found in IBD and non-IBD colonic biopsies, demonstrating increased CD45+ cells in IBD biopsies (**Fig. S2A**). Next, we assessed response of immune cells to dietary fibers using THP-1-derived macrophages and primary peripheral blood mononuclear cells (PBMC). Inulin and FOS, but not barley β -D-glucan, maltodextrin, or starch, induced IL-1 β secretion by THP-1 macrophages, comparable to previously studied fungal β -(1,3)glucans (zymosan, curdlan; **Fig. 1A**). Similar results were demonstrated in PBMCs from healthy donors (**Fig. 1B**). To address the possibility that free fructose could drive this effect,¹⁷ we determined the concentration of fructose within the fiber solutions and showed that IL-1 β production was not increased by THP-1 macrophages with the same fructose concentrations (**Fig. S2B**). Leukocytes were confirmed to be present in the luminal mucus layer, particularly in IBD patients, supporting the potential for direct physiological interaction with luminal fibers (**Fig. S2C**). Colonic biopsies from pediatric non-IBD (*n*=19), CD (*n*=33), and UC (*n*=13) patients were cultured *ex vivo* with no fiber (NF) or FOS (5mg/mL; 24hrs). FOS increased pro-inflammatory interleukin (IL)-1 β secretion by a mean of 75% (CD active; *p*<0.05)

and 105% (UC active; $p < 0.05$) compared to NF, and to a lesser extent in biopsies from remission IBD patients (**Fig. 1C-D**). Conversely, IL-1 β was decreased by 40% ($p < 0.05$) in non-IBD control biopsies exposed to FOS.

β -fructans induced specific inflammatory pathways and altered epithelial barrier

Human cytokine gene arrays of pediatric patient biopsies, cultured *ex vivo* with FOS or NF, identified broad FOS-induced pro-inflammatory pathways (*e.g.*, *CX3CR1*, *IL8*, *IL1B*, *NFKB1*), but the magnitude or direction varied, depending on IBD activity (**Fig. S3A**). Distinct gene expression footprints were identified in B cell, T cell, and macrophage cell lines (**Fig. S3B**). Top genes of interest in *ex vivo* biopsy response to FOS were identified (fold change > 1.5 versus NF; $p < 0.25$) and literature review of STRING analysis (ELIXIR) targets demonstrated that targets increased in response to FOS in pediatric IBD patient biopsies were linked to inflammation and epithelial barrier integrity (**Fig. S3C**).¹⁸⁻²⁷ Gene targets of interest (*IL1 β* , *CX3CL1*, *IL23A*, *NLRP3*) were validated by RT-qPCR in 35 pediatric patient biopsies cultured *ex vivo* and various cell lines, cultured with fibers, demonstrating that pro-inflammatory markers were increased in active IBD patient biopsies in response to FOS compared to non-IBD, mostly driven by myeloid cells (**Fig. S3D**).

Pathways associated with the epithelial barrier (*e.g.*, IL-23, STAT3, CCL3) were examined by assessing fiber effects on different physical properties (**Table S1**) in an *in vitro* epithelial monolayer model. We found fiber type-specific effects on epithelial barrier formation, possibly further impacting IBD pathogenesis (**Fig. S4**). Inulin Sigma (chicory root; $p < 0.0001$), inulin High Performance (HP; chicory root; $p < 0.001$), and maltodextrin ($p < 0.01$) improved epithelial barrier formation, while β -D-glucan isolated from barley diminished barrier formation ($p < 0.0001$) in T84 intestinal epithelial cells; FOS did not significantly alter barrier formation. Interestingly, inulin purity and polymerization appeared to relate to differences in its effect on barrier formation as we examined two inulin compounds, both sourced from chicory root (**Table S1**); inulin HP (DP 25, 99.5%) significantly increased barrier formation compared to inulin Sigma (DP 12, 92%; $p < 0.05$).

To expand on fiber-mediated inflammatory effects, secreted cytokines associated with identified pathways (IL-1 β , IL-23, MIP-1 α , IL-5) were validated by multiplex ELISA (MesoScale Discovery; MSD) using supernatants from 40 pediatric patient *ex vivo* biopsy cultures (**Fig. 2A**). To better examine the subset of patients observed to experience pro-inflammatory response to FOS, pediatric patients were defined as pro-inflammatory responders (IBD-R) or non-responders (IBD-NR), based on *ex vivo* biopsy inflammatory response to FOS (IBD-R: IL-1 β fold increase > 1.1 vs NF defined as responder). We observed a significant increase in IL-1 β , IL-23, and IL-5 secretion, but not MIP-1 α in IBD-R, compared to IBD-NR (**Fig. 2A**). We further validated these cytokines significantly increased in response to FOS in THP-1 macrophages (**Fig. 2B**) and PBMCs (**Fig. 2C**), compared to no fiber (NF).

FOS promoted inflammation via the NLRP3 and TLR2 pathways

As we had identified a number of NLRP3 pathway targets associated with response to FOS, we utilized NLRP3 inflammasome inhibitors (Ac-YVAD-cmk, glyburide, and MCC950) with positive control activator (ATP) or FOS

in THP-1 macrophages to assess the role of NLRP3 (**Fig. 2D**). We found that inhibition of NLRP3 significantly reduced IL-1 β secretion in response to FOS (glyburide and MCC950) and ATP (YVAD and MCC950). We next treated THP-1 macrophages with a series of fibers, with or without MCC950 and showed that inhibition of NLRP3 significantly reduced pro-inflammatory response (IL-1 β secretion) to zymosan, curdlan, and FOS (**Fig. 2E**). In PBMCs, inhibition of NLRP3 also reduced pro-inflammatory response (IL-1 β and IL-23 secretion) to FOS (**Fig. 2F**). Prior research using basic molecular modeling suggests that TLR2 may serve as a receptor for β -fructans;¹⁶ therefore, we conducted improved comprehensive docking prediction of the kestose-1 molecule, a precursor and structural representative of β -fructan, on the following heterodimers: TLR1-TLR2 (PDB ID: 2Z7X) and TLR2-TLR6 (PDB ID: 3A79) (**Fig. 2G-H**).^{28, 29} A known ligand (Pam3CSK4) has been shown to bridge the ectodomains and stabilize the TLR1-TLR2 heterodimer through hydrophobic, hydrogen-bonding, and electrostatic interactions.²⁸ The interactions of Pam3CSK4 occur along the TLR1-TLR2 interface, containing the long and continuous lipid-binding site formed in conjunction with the TLR1 channel and the TLR2 pocket.²⁸ The region of the TLR1-TLR2 interface which forms hydrophilic interactions with Pam3CSK4 corresponded to the best predicted poses of kestose-1 (**Fig. 2G**). For the TLR2-TLR6 heterodimer, a similar ligand (Pam2CSK4) interacts with the TLR2 pocket which induces dimerization.²⁹ Unlike Pam3CSK4, Pam2CSK4 does not extend into the TLR6 channel. Again, the best predicted poses of kestose-1 for the TLR2-TLR6 heterodimer are found near the TLR2 pocket, but not within the TLR6 channel (**Fig. 2H**). Inhibition of TLR2 in THP-1 macrophages significantly reduced pro-inflammatory response (IL-1 β secretion) to zymosan and FOS (**Fig. 2I**), while in PBMCs inhibition of TLR2 significantly reduced the FOS-induced pro-inflammatory response (IL-1 β and IL-23 secretion; **Fig. 2J**). Together, these findings support a direct interaction between β -fructan and TLR2 driving pro-inflammatory response through the NLRP3 inflammasome pathway.

FOS fermentation reduces inflammation

To examine the link between microbiota composition or function and fermentation, we collected whole microbiota colonic intestinal mucosal washes from pediatric non-IBD and IBD patients during colonoscopy. Washes were cultured anaerobically with NF or FOS for 24 hrs, followed by centrifugation to remove microbes; supernatants were collected. THP-1 macrophages were then incubated with these supernatants, or with NF or FOS alone. Unfermented FOS and ATP (positive control) increased IL-1 β (**Fig. 3A**; left panel). NF supernatants, which included the natural fermentation products of patient microbes, increased IL-1 β secretion (right panel). Although microbes were removed by centrifugation, these post-fermentation supernatants likely contained secretions from microbe cultures, which could increase IL-1 β . Supporting our hypothesis, fermentation of FOS with whole intestinal wash microbes from non-IBD or IBD remission/mild patients reduced IL-1 β secretion in macrophages, but microbes from IBD patient with active disease (biopsies were collected from normal-appearing bowel) did not (**Fig. 3A**; far right), likely due to an impaired ability of the microbial community to ferment FOS. A positive correlative trend was found between IL-1 β secreted from FOS-treated patient biopsies (shown in **Fig. 1C**) and IL-1 β secreted from THP-1

macrophages, treated with matching patient microbe fermentation supernatants ($R^2=0.3633$; $p=0.08$; **Fig. 3B**), further supporting changes in microbe-mediated fermentation drive the pro-inflammatory response to FOS.

We next examined production of SCFA (*e.g.*, acetate, propionate, butyrate) in the patient whole microbiota fiber fermentation supernatants described above. Acetate levels in fermentation supernatants (**Fig. S5A**) correlated positively with THP-1 macrophage secretion of IL-1 β in response to fermentation supernatants in both non-IBD patients and IBD-R, but not in IBD-NR. Propionate and butyrate negatively correlated with THP-1 macrophage secretion of IL-1 β in response to FOS fermentation supernatants in both non-IBD and IBD-R. This links FOS fermentation and SCFA production in prevention of inflammatory response to dietary fibers. The amount of fiber remaining in these fermentation supernatants was also evaluated, demonstrating a near-complete breakdown of β -fructan (FOS and inulin) following fermentation with microbes from non-IBD patients (average 0.5mg/mL remaining), versus approximately 50% average fermentation following fermentation with microbes from responder IBD patients (average 2.5-5mg/mL remaining; **Fig. S5B**).

Shotgun metagenomics of intestinal washes (those used for fermentation cultures) demonstrated an expected level of variability among pediatric patients (**Fig. S6**). At the phylum level, Firmicutes were decreased in CD (29.72% vs. 39.66% in non-IBD); Actinobacteria were increased in UC (14.19% vs. 5.44% in non-IBD; $p<0.05$). Patients with active CD displayed increased Proteobacteria (38.25% vs. 4.12% in non-IBD; $p<0.05$). At the species level (**Table S2**), *Parabacteroides distasonis* was lower in CD (0.14%; $p<0.05$) and UC (0.37%; $p<0.05$), compared to non-IBD (2.00%). *Bacteroides stercoris* was also reduced in CD (0.03% vs. 1.27% in non-IBD; $p<0.05$).

Random forest classification trained on microbial functions (enzyme abundances by metagenomics), correlating biopsy response to FOS with matching microbe composition and function, predicted response (IBD-R vs IBD-NR) to FOS (**Fig. 3C**); receiver-operating characteristic (ROC) curve, indicated an acceptable diagnostic potential (ROC-AUC=0.7; **Fig. 3D**). Ten enzymes with the highest predictive value were identified (**Fig. 3E**). Of those, Riboflavin synthase, Glucosylceramidase, β -lactamase, 3-dehydro-L-gulonate 2-dehydrogenase, and Adenine phosphoribosyltransferase were increased in the IBD-NR, while UDP-N-acetylglucosamine 2-epimerase was increased in IBD-R (**Fig. 3C**). In contrast to function, microbial composition alone could not predict patient response to FOS, based on the random forest classification model (out-of-bag error rate >0.7). These data indicate that gut microbial function (not composition) predicts patient pro-inflammatory response to FOS, supporting our hypothesis that overall community function impacts fiber fermentation and affects associated pro-inflammatory effects.

We were further able to support these findings by treating THP-1 macrophages with physiologically relevant concentrations of SCFA and FOS, identified in **Fig. S5**, following fermentation with IBD-NR (black) or IBD-R (grey) patient microbe cultures (**Fig. 3F**). Significantly less IL-1 β was secreted following treatment of THP-1 with the concentration of FOS remaining, following fermentation with IBD-NR microbes (0.5 mg/mL FOS), compared to IBD-R (5 mg/mL FOS). Addition of SCFA concentrations produced following FOS fermentation by microbes from either IBD-NR or IBD-R significantly dampened inflammatory effect (reduced THP-1 macrophage IL-1 β secretion) of their respective FOS fermentation concentrations (IBD-NR 0.5mg/mL FOS; IBD-R 5mg/mL FOS). Only the combination of

reduced FOS and specific production of SCFA from fermentation by IBD-NR microbes was able to entirely negate the pro-inflammatory effect of FOS.

Patterns of microbes presently known to be involved in fiber fermentation in published reports (**Table S3**; *e.g.*, Faecalibacterium, Roseburia, Bifidobacterium, Bacteroides) were associated with disease states (**Fig. S6D**), supporting that clusters of microbes known to be essential for fiber fermentation and SCFA production are typically reduced or altered in IBD patients.³⁰ Taken together, metagenomics suggests that specific microbe community fiber fermentation functional deficiencies could explain the observed pro-inflammatory response to fiber in IBD patients with active disease.

Pro-inflammatory responses to β -fructan confirmed in a randomized control trial (RCT) of UC patients in remission

We recently completed an RCT, aimed to assess the efficacy of β -fructans (FOS and inulin) in preventing relapse in adult UC patients in symptomatic remission.¹² While our findings showed a positive impact of β -fructans in many patients in remission, significantly reducing the risk of biochemical relapse (defined as fecal calprotectin > 200) compared to placebo, we also demonstrated that β -fructans (15g/day over 6 months) could not prevent symptomatic relapses in UC patients in remission; in fact, 31% of individuals in the β -fructans group versus 24% (NS) in the placebo group experienced symptomatic relapse at the study endpoint in this cohort of UC patients.¹² These data support the benefits of β -fructans while also demonstrating the potential negative impacts in select IBD patients, even in remission. There are clear differences between CD and UC, and between IBD patients diagnosed as very early onset (<6 years), pediatric (6-18 years), and adult (>18 years), indicating potential differences between our pediatric population and adult RCT cohort in this study. Nevertheless, we were able to use this RCT cohort to validate that cytokines (IL-1 β , IL-23, IL-5) associated with pro-inflammatory response to β -fructans in select IBD patients (identified in **Fig. 1-2**) were also increased in intestinal biopsy lysates from the RCT cohort, but only in UC patients who flared following consumption of β -fructans, and not in the placebo arm (**Fig. 4A**). These results further confirmed the pro-inflammatory response to β -fructans in select IBD patients, supporting the clinical relevance of our *ex vivo* biopsy findings.

Furthermore, examining the microbial enzyme pathways identified in **Fig 3C**, we found that riboflavin, which was reduced in patients who displayed a pro-inflammatory response to β -fructans in our *ex vivo* patient biopsy model, was also significantly lower in baseline stool samples collected only from patients in the β -fructan RCT¹² who relapsed in response to β -fructan consumption (**Fig 4B**). Riboflavin negatively correlated with fecal calprotectin (gut inflammation marker) fold-change from baseline to month-6 (**Fig. 4C**) in this RCT; riboflavin was not predictive of relapse in placebo RCT patients.

Fiber avoidance correlated with inflammation

Given reported reduced consumption of dietary fibers in IBD patients,³¹ we used food frequency questionnaires (FFQ; reflecting previous diet) to calculate consumption of approximate daily dietary fiber intake (inulin, FOS, pectin,

and β -D-glucan), using a fiber content database (**Table S4**). Despite variability in consumption of dietary fibers, pediatric IBD patients with active disease consumed significantly less β -D-glucan compared to patients in remission (**Fig. S7A**; $p < 0.05$). Supporting our hypothesis, we found significantly lower FOS consumption in pediatric patients with matching pro-inflammatory biopsy responses to FOS (IBD-R), compared to IBD-NR (**Fig. S7B**; $p < 0.01$); FOS consumption negatively correlated with IL-1 β secretion in response to FOS in matching pediatric biopsies (**Fig. S7C**). While these findings do not prove causality, they support a link between intestinal pro-inflammatory response to fiber and dietary fiber avoidance in pediatric IBD.

Discussion

IBD patients describe variable intolerance of fiber consumption,⁸ which can lead to avoidance of generally beneficial fibers and worse patient outcomes.⁹⁻¹¹ We utilised IBD as a model to confirm our hypothesis that fibers that remain unfermented could drive inflammation. Supporting our findings, β -fructans have been shown to induce reactive oxygen species (ROS) production and associated inflammation, possibly through NLRP3 signalling³² and clinical studies show that FOS consumption can worsen outcomes in select patients.^{5,12} Nevertheless, the potentially negative effects of dietary fibers are poorly documented and usually overlooked.

Here, unfermented FOS induced pro-inflammatory cytokines in PBMCs, THP-1 macrophages, and IBD patient biopsies cultured *ex vivo*, via pathways previously associated with IBD including TLR2 and NLRP3, which are known to cooperate in response to ligand stimuli such as lipopolysaccharide (LPS).^{33,34} This was confirmed in select IBD patients in an RCT inulin/FOS-treated cohort.¹² We propose that interactions between unfermented fibers in the luminal contents with leukocytes found in the mucosal lining or lamina propria exposed due to epithelial barrier breakdown, could drive these responses in a physiological setting. TLR2 is differentially expressed in cell types, with greater levels in monocytes and macrophages, supporting increased potential for interaction between unfermented β -fructans and TLR2 in IBD patients where these cell populations are increased, particularly in patients with active disease. Response could be explained further by the increased presence of inflammatory macrophages in inflamed tissues of IBD patients although the presence of specific macrophage populations was not examined in this study.³⁵ The epithelial barrier, which typically prevents undesired immune interaction with luminal content, is commonly disrupted in IBD.³⁶ Here, β -fructans improved barrier formation *in vitro*, while β -D-glucan reduced barrier formation, possibly due to structural differences between β -fructans and β -D-glucan.² Our data support future investigation of these pathways using organoid and animal models which would provide more mechanistic findings in relation to the effects of these fibers on epithelial barrier integrity.

Sensitivity to fibers was further supported by our findings that patients with active disease (IBD-R) consumed less dietary fiber than patients in remission (IBD-NR), and lower FOS consumption (measured by FFQ) correlated with higher pro-inflammatory response to FOS in matching patient biopsies cultured *ex vivo*. This suggests that patients with fiber sensitivities might unknowingly avoid consumption of select FOS-containing foods, possibly in attempts to ameliorate symptoms.

Microbial function was predictive of response to FOS in patient samples. The enzyme UDP-N-acetylglucosamine was increased in IBD-R, suggesting that this pathway may be involved in the pro-inflammatory response to fibers, possibly via T-cell activation.³⁷ In contrast, IBD-R had significantly reduced riboflavin synthase which displays anti-inflammatory, antioxidant, and microbe-altering properties in IBD patients.³⁸ Both riboflavin synthase and glucosylceramidase inhibit a variety of pro-inflammatory cytokines (IL-6, TNF, IL-1 β).³⁹ Riboflavin (vitamin B2) was lower in stool of UC patients in our RCT who flared following 6-month consumption of β -fructans and its absence correlated with increased fold-change in fecal calprotectin, suggesting further links between riboflavin and response to fiber consumption in IBD patients. *Faecalibacterium prausnitzii* is thought to use riboflavin as a mediator of butyrate and SCFA production,⁴⁰ suggesting a key link between fiber-fermenting microbes, enzyme abundance, SCFA production, and inflammatory response to dietary fibers.

IBD-R mucosal microbiota washes produced increased acetate and decreased propionate and butyrate through fermentation of FOS. Acetate is known to increase ROS production in macrophages, while butyrate and propionate inhibit inflammation through various pathways,⁴¹ suggesting that even when fermentation is not reduced, altered production of SCFA may promote inflammation. While no individual microbe species associated explicitly with pro-inflammatory response to FOS, there were altered patterns of microbial species abundances that may help identify microbiome changes associated with altered fermentation. Abundance of microbes known to ferment fibers² was significantly reduced in moderate and severe CD patients; particularly, the dominant fiber-fermenting and butyrate-producing microbes *Roseburia hominis* and *F. prausnitzii*, as expected.^{2, 42} While recent studies have indicated the importance of these mucosal microorganisms in the gut ecosystem and in relation to diet, there is only limited research on the interactions of diet with mucosal microbiota in IBD.

It is important to note some limitations of our study. While we confirmed the purity of the fibers used with low LPS (within test limits of detection), other microbial contaminants may co-purify with the three β -fructans (FOS/inulin) from chicory roots used in this study, along with other fibers. Further, samples were collected following colonoscopy preparation, which is known to alter microbiota composition; while our main focus was on mucosa-associated microbes, which are less impacted by bowel prep, luminal microbiota also play an important role in fibre fermentation. Mucosal microbes typically include important fiber fermenting microbes (*Bacteroidetes*, *Firmicutes* [*Veillonellaceae*, *Ruminococcaceae*]) compared to stool microbiota; however, our understanding of the precise community of microbes (luminal or mucosal) involved in fiber fermentation remains limited by our ability to culture and identify these microbes.^{2, 43}

We propose that when fiber-fermenting microbes are present in the gut, and normal barrier integrity prevents interactions between fibers and underlying immune cells, fermentation of select fibers enhances the barrier and reduces inflammatory response. In contrast, select disease state scenarios, such as active IBD, provide conditions leading to increased exposure and sensitivity to unfermented dietary fibers to develop in the diseased gut microenvironment. These conditions include 1) a reduced abundance and capacity of the gut microbiota to ferment fiber, 2) increased presence of immune cells at the mucosal surface, and 3) inflammatory damage to the

gut barrier. Interaction of FOS and inulin with host cells could then result in gut inflammation through direct effects of intact fiber and/or altered SCFA production. Our work could have significant impacts on patient care. Further clinical studies are warranted to determine if FOS should be avoided by IBD patients when experiencing specific alterations in gut microbiota composition and functions, specifically associated with lack of fermentation, especially with active disease. Since altered microbiota is more frequently found in active IBD patients, it could be speculated that FOS (and potentially other fibers) should be administered as adjunct therapy only after medical therapy has induced remission (with barrier repair/mucosal healing and healthy microbiota functions) in these individuals, to ensure the other benefits of fibers and their products.

Figure Legend

Figure 1: Unfermented dietary FOS induces a pro-inflammatory immune response in THP-1 macrophages, PBMC's, and patient biopsy tissues cultured *ex vivo*. ELISA for secreted IL-1 β (marker of inflammation; supernatants) was performed in (A) THP-1 macrophages in response to starch (S), ATP, no fiber (NF), maltodextrin (M), zymosan (Z), curdlan (C), oat β -D-glucan (B), inulin (I), or FOS, stimulated for 24hr, (B) human PBMC in response to NF, maltodextrin, zymosan, and FOS, and (C-D) pediatric non-IBD (n=19), CD (n=33), and UC (n=13) patient biopsies cultured *ex vivo* with NF or oligofructose (FOS; 5 mg/mL) for 24 hr. Results are displayed as (C) fold change in FOS/NF secretion for individual patients for ease of comparison, or (D) paired raw IL-1 β secretions from biopsy tissues (decreased [blue] and increased [red] IL-1 β secretion; FOS vs NF). *p<0.05, **p<0.01, ***p<0.001, ****p<0.0001.

Figure 2: A prototypical pro-inflammatory response to is driven through NLRP3 and TLR2. Multiplex ELISA (MSD) was used to measure secretion of pro-inflammatory cytokines in response to FOS (5mg/mL) versus NF in (A) *ex vivo* biopsy secretions, in non-IBD (n=12), IBD nonR [CD nonR (n=6), UC nonR (4)], and IBD R [CD R (n=9), and UC R (n=5)] patient biopsies, (B) THP-1 macrophages, and (C) PBMCs (n=6). (D) ELISA of secreted IL-1 β was performed in supernatants from THP-1 macrophages treated with NF, FOS, or ATP control with the addition of the NLRP3 inhibitors Ac-YVAD-cmk (50 μ M), glyburide (200 μ M), or MCC950 (1 μ M). Effect of inhibition of NLRP3 (MCC950) on cytokine secretion in response to indicated fibers was measured by MSD in (E) THP-1 macrophages and (F) PBMCs. (G) TLR1(cyan)-TLR2(magenta) heterodimer with top 35 docked kestose-1 (represents β -fructan) poses (*e.g.*, arrows) aligned and overlaid on the TLR1-TLR2 (PDB ID: 2Z7X) structure represents all poses with a predicted binding free energy < -6kJ/mol and maximum -7.48kJ/mol. (H) TLR2(magenta)-TLR6(blue) heterodimer with the top 52 docked kestose-1 poses (*e.g.*, arrows) aligned and overlaid on the TLR2-TLR6 (PDB ID: 3A79) structure represents all poses with a predicted binding free energy < -6kJ/mol and maximum -7.39kJ/mol. Effect of inhibition of TLR2 (inh-c29; 75 μ M) on cytokine secretion in response to indicated fibers was measured by MSD in (I) THP-1 macrophages and (J) PBMCs. *p<0.05, **p<0.01, ***p<0.001, ****p<0.0001. IBD rem (remission); Bc (B Cell); Tc (T cell); M ϕ (macrophage). Pro-inflammatory responders (IBD-R: IL-1 β fold increase >1.1 vs NF; ELISA Fig 1A) or non-responders (IBD-NR).

Figure 3: IBD patient microbial consortia fermentation function correlates with fiber-mediated immune response. (A) Pediatric non-IBD (n=8), IBD remission (n=4), IBD mild (n=6), or IBD moderate/severe (n=4) patient intestinal wash samples were collected during colonoscopy; total microbe wash was incubated with NF or FOS to create a whole microbe fermentation solution from each patient. These solutions were then incubated with macrophages and compared to NF (red dot line) or FOS alone by measuring IL-1 β secretion by ELISA. (B) Results from non-IBD (grey), remission/mild IBD (black), and moderate/severe IBD (red) biopsies and washes calculated as the ratio of FOS/NF for each patient were compared and statistically evaluated by Kendall ranking. (C) Relative enzyme abundance in biopsy FOS responder (n=8) and non-responder (n=9) cohorts determined by metagenomics. (D) ROC-AUC and random forest classification demonstrate an ability of enzyme abundance to predict response to FOS in patient biopsies. (E) Random forest analysis identifies the top 10 enzymes that contribute the most to the fermentation effect. (F) THP-1 macrophages were cultured with SCFA (acetate, butyrate, propionate) or in combination with FOS at levels following fermentation by responder microbiota (5 mg/ml) or non-responder (0.5 mg/ml). *p<0.05, **p<0.01, ***p<0.001.

Armstrong *et al.* 2022

Figure 4: Pro-inflammatory response to consumption of β -fructans was confirmed in a randomized control trial cohort. (A) Multiplex ELISA of UC patient biopsy lysates from a prebiotic RCT including placebo remission (Pc rem n=11), placebo flare (Pc flare n=10), β -fructan remission (β rem n=10), β -fructan flare (β flare n=7). **(B)** Riboflavin (baseline) and **(C)** fecal calprotectin (month 6 vs baseline) were measured in stool from a prebiotic RCT in UC patients, including placebo remission (n=11), placebo flare (n=10), β -fructan remission (n=10), β -fructan flare (n=7) and were correlated against one another using linear regression modeling. * $p < 0.05$, **** $p < 0.0001$.

Journal Pre-proof

References

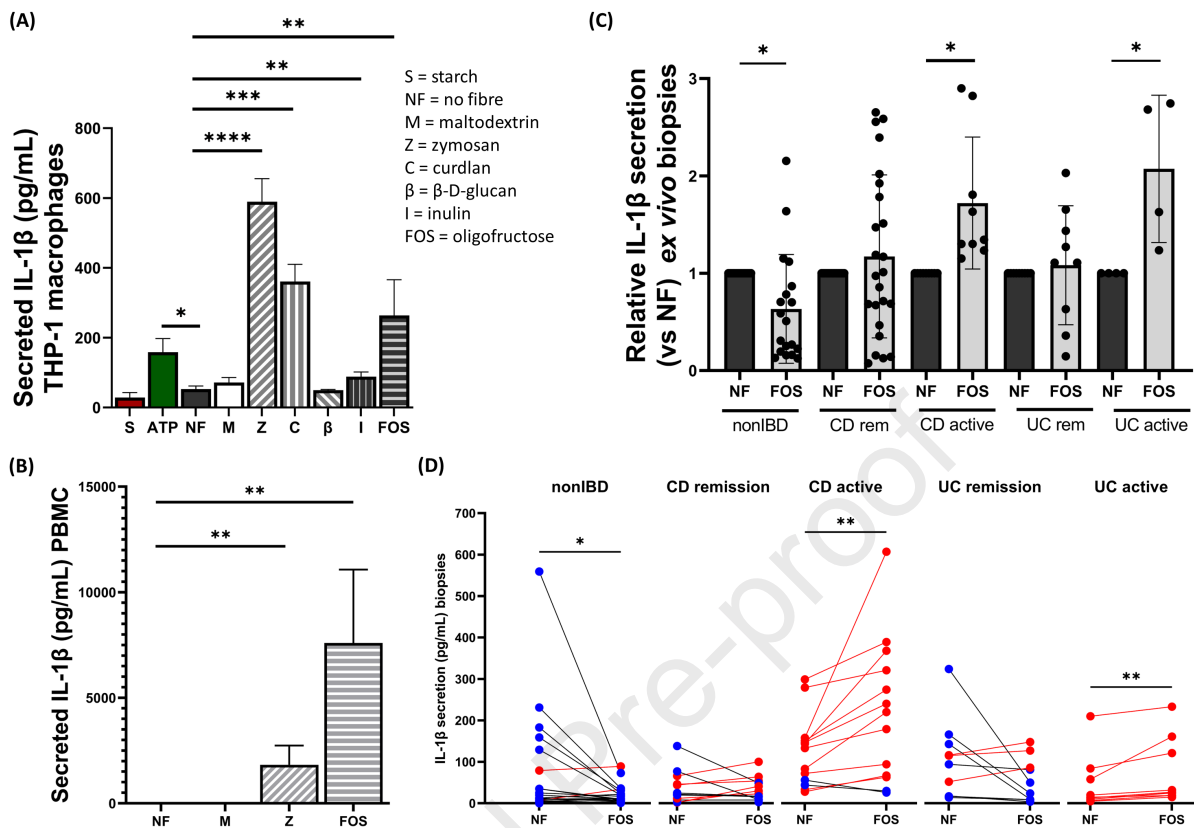
1. Sonnenburg ED, Sonnenburg JL. Starving our microbial self: the deleterious consequences of a diet deficient in microbiota-accessible carbohydrates. *Cell Metab* 2014;20:779-786.
2. Armstrong H, Mander I, Zhang Z, et al. Not all fibres are born equal; variable response to dietary fibre subtypes in IBD. *Frontiers in Pediatrics* 2021;8.
3. Rios-Covian D, Ruas-Madiedo P, Margolles A, et al. Intestinal Short Chain Fatty Acids and their Link with Diet and Human Health. *Front Microbiol* 2016;7:185.
4. Heinsbroek SE, Williams DL, Welting O, et al. Orally delivered beta-glucans aggravate dextran sulfate sodium (DSS)-induced intestinal inflammation. *Nutr Res* 2015;35:1106-12.
5. Benjamin JL, Hedin CR, Koutsoumpas A, et al. Randomised, double-blind, placebo-controlled trial of fructo-oligosaccharides in active Crohn's disease. *Gut* 2011;60:923-9.
6. Machiels K, Joossens M, Sabino J, et al. A decrease of the butyrate-producing species *Roseburia hominis* and *Faecalibacterium prausnitzii* defines dysbiosis in patients with ulcerative colitis. *Gut* 2014;63:1275-83.
7. Valcheva R, Koleva P, Martinez I, et al. Inulin-type fructans improve active ulcerative colitis associated with microbiota changes and increased short-chain fatty acids levels. *Gut Microbes* 2019;10:334-357.
8. Cohen AB, Lee D, Long MD, et al. Dietary patterns and self-reported associations of diet with symptoms of inflammatory bowel disease. *Dig Dis Sci* 2013;58:1322-8.
9. Nieves R, Jackson RT. Specific carbohydrate diet in treatment of inflammatory bowel disease. *Tenn Med* 2004;97:407.
10. Grammatikopoulou MG, Goulis DG, Gkiouras K, et al. Low FODMAP Diet for Functional Gastrointestinal Symptoms in Quiescent Inflammatory Bowel Disease: A Systematic Review of Randomized Controlled Trials. *Nutrients* 2020;12.
11. Knight-Sepulveda K, Kais S, Santaolalla R, et al. Diet and Inflammatory Bowel Disease. *Gastroenterol Hepatol (N Y)* 2015;11:511-20.
12. Valcheva R, Armstrong H, Kovic O, et al. Double blind placebo-controlled trial for the prevention of ulcerative colitis relapses by β -fructan prebiotics: efficacy and metabolomic analysis. *medRxiv* 2022:2022.01.16.22269376.
13. Ohman T, Teirila L, Lahesmaa-Korpinen AM, et al. Dectin-1 pathway activates robust autophagy-dependent unconventional protein secretion in human macrophages. *J Immunol* 2014;192:5952-62.
14. Tsoni SV, Brown GD. beta-Glucans and dectin-1. *Ann N Y Acad Sci* 2008;1143:45-60.
15. Ortega-Gonzalez M, Ocon B, Romero-Calvo I, et al. Nondigestible oligosaccharides exert nonprebiotic effects on intestinal epithelial cells enhancing the immune response via activation of TLR4-NFkappaB. *Mol Nutr Food Res* 2014;58:384-93.
16. Fernandez-Lainez C, Akkerman R, Oerlemans MMP, et al. beta(2-->6)-Type fructans attenuate proinflammatory responses in a structure dependent fashion via Toll-like receptors. *Carbohydr Polym* 2022;277:118893.
17. Montrose DC, Nishiguchi R, Basu S, et al. Dietary Fructose Alters the Composition, Localization, and Metabolism of Gut Microbiota in Association With Worsening Colitis. *Cell Mol Gastroenterol Hepatol* 2021;11:525-550.
18. Grondin JA, Kwon YH, Far PM, et al. Mucins in Intestinal Mucosal Defense and Inflammation: Learning From Clinical and Experimental Studies. *Front Immunol* 2020;11:2054.
19. Panda SK, Wigerblad G, Jiang L, et al. IL-4 controls activated neutrophil FcgammaR2b expression and migration into inflamed joints. *Proc Natl Acad Sci U S A* 2020;117:3103-3113.

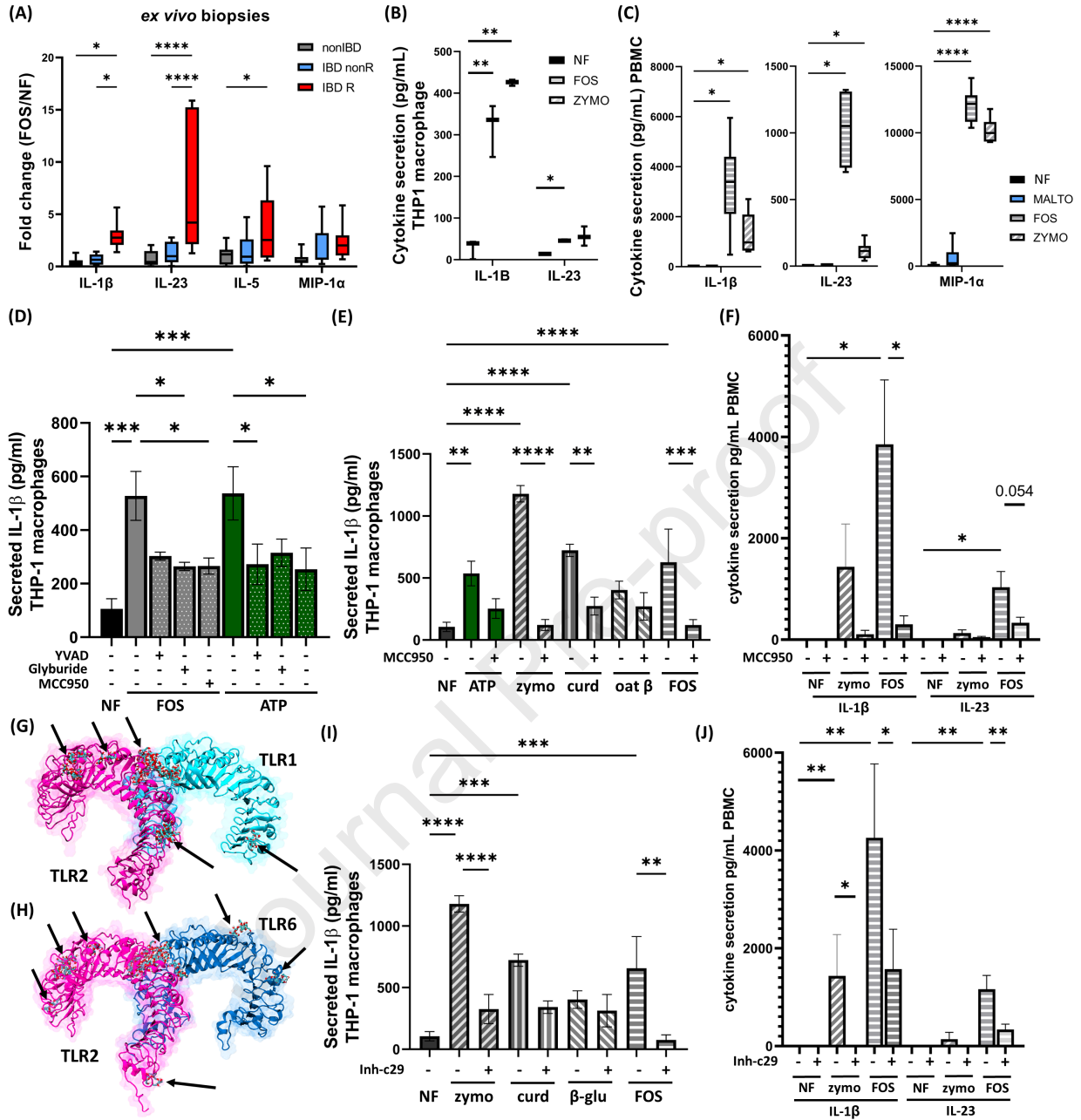
20. Kazanietz MG, Durando M, Cooke M. CXCL13 and Its Receptor CXCR5 in Cancer: Inflammation, Immune Response, and Beyond. *Front Endocrinol (Lausanne)* 2019;10:471.
21. Zhen Y, Zhang H. NLRP3 Inflammasome and Inflammatory Bowel Disease. *Front Immunol* 2019;10:276.
22. Mao L, Kitani A, Strober W, et al. The Role of NLRP3 and IL-1beta in the Pathogenesis of Inflammatory Bowel Disease. *Front Immunol* 2018;9:2566.
23. Al-Sadi RM, Ma TY. IL-1beta causes an increase in intestinal epithelial tight junction permeability. *J Immunol* 2007;178:4641-9.
24. Lerch MM, Conwell DL, Mayerle J. The anti-inflammasome effect of lactate and the lactate GPR81-receptor in pancreatic and liver inflammation. *Gastroenterology* 2014;146:1602-5.
25. Maroni L, Agostinelli L, Saccomanno S, et al. Nlrp3 Activation Induces IL-18 Synthesis and Affects the Epithelial Barrier Function in Reactive Cholangiocytes. *Am J Pathol* 2017;187:366-376.
26. Mabuchi T, Chang TW, Quinter S, et al. Chemokine receptors in the pathogenesis and therapy of psoriasis. *J Dermatol Sci* 2012;65:4-11.
27. Imai T, Yasuda N. Therapeutic intervention of inflammatory/immune diseases by inhibition of the fractalkine (CX3CL1)-CX3CR1 pathway. *Inflamm Regen* 2016;36:9.
28. Jin MS, Kim SE, Heo JY, et al. Crystal structure of the TLR1-TLR2 heterodimer induced by binding of a tri-acylated lipopeptide. *Cell* 2007;130:1071-82.
29. Kang JY, Nan X, Jin MS, et al. Recognition of lipopeptide patterns by Toll-like receptor 2-Toll-like receptor 6 heterodimer. *Immunity* 2009;31:873-84.
30. Deleu S, Machiels K, Raes J, et al. Short chain fatty acids and its producing organisms: An overlooked therapy for IBD? *EBioMedicine* 2021;66:103293.
31. Davis R, Day A, Barrett J, et al. Habitual dietary fibre and prebiotic intake is inadequate in patients with inflammatory bowel disease: findings from a multicentre cross-sectional study. *J Hum Nutr Diet* 2021;34:420-428.
32. Singh V, Yeoh BS, Walker RE, et al. Microbiota fermentation-NLRP3 axis shapes the impact of dietary fibres on intestinal inflammation. *Gut* 2019;68:1801-1812.
33. Zhang J, Fu S, Sun S, et al. Inflammasome activation has an important role in the development of spontaneous colitis. *Mucosal Immunol* 2014;7:1139-50.
34. Coccia M, Harrison OJ, Schiering C, et al. IL-1beta mediates chronic intestinal inflammation by promoting the accumulation of IL-17A secreting innate lymphoid cells and CD4(+) Th17 cells. *J Exp Med* 2012;209:1595-609.
35. Flo TH, Halaas O, Torp S, et al. Differential expression of Toll-like receptor 2 in human cells. *J Leukoc Biol* 2001;69:474-81.
36. Turpin W, Lee SH, Raygoza Garay JA, et al. Increased Intestinal Permeability Is Associated With Later Development of Crohn's Disease. *Gastroenterology* 2020;159:2092-2100 e5.
37. Li Y, Xie M, Men L, et al. O-GlcNAcylation in immunity and inflammation: An intricate system (Review). *Int J Mol Med* 2019;44:363-374.
38. von Martels JZH, Bourgonje AR, Klaassen MAY, et al. Riboflavin Supplementation in Patients with Crohn's Disease [the RISE-UP study]. *J Crohns Colitis* 2020;14:595-607.
39. Menezes RR, Godin AM, Rodrigues FF, et al. Thiamine and riboflavin inhibit production of cytokines and increase the anti-inflammatory activity of a corticosteroid in a chronic model of inflammation induced by complete Freund's adjuvant. *Pharmacol Rep* 2017;69:1036-1043.
40. Soto-Martin EC, Warnke I, Farquharson FM, et al. Vitamin Biosynthesis by Human Gut Butyrate-Producing Bacteria and Cross-Feeding in Synthetic Microbial Communities. *mBio* 2020;11.
41. Li M, van Esch B, Wagenaar GTM, et al. Pro- and anti-inflammatory effects of short chain fatty acids on immune and endothelial cells. *Eur J Pharmacol* 2018;831:52-59.

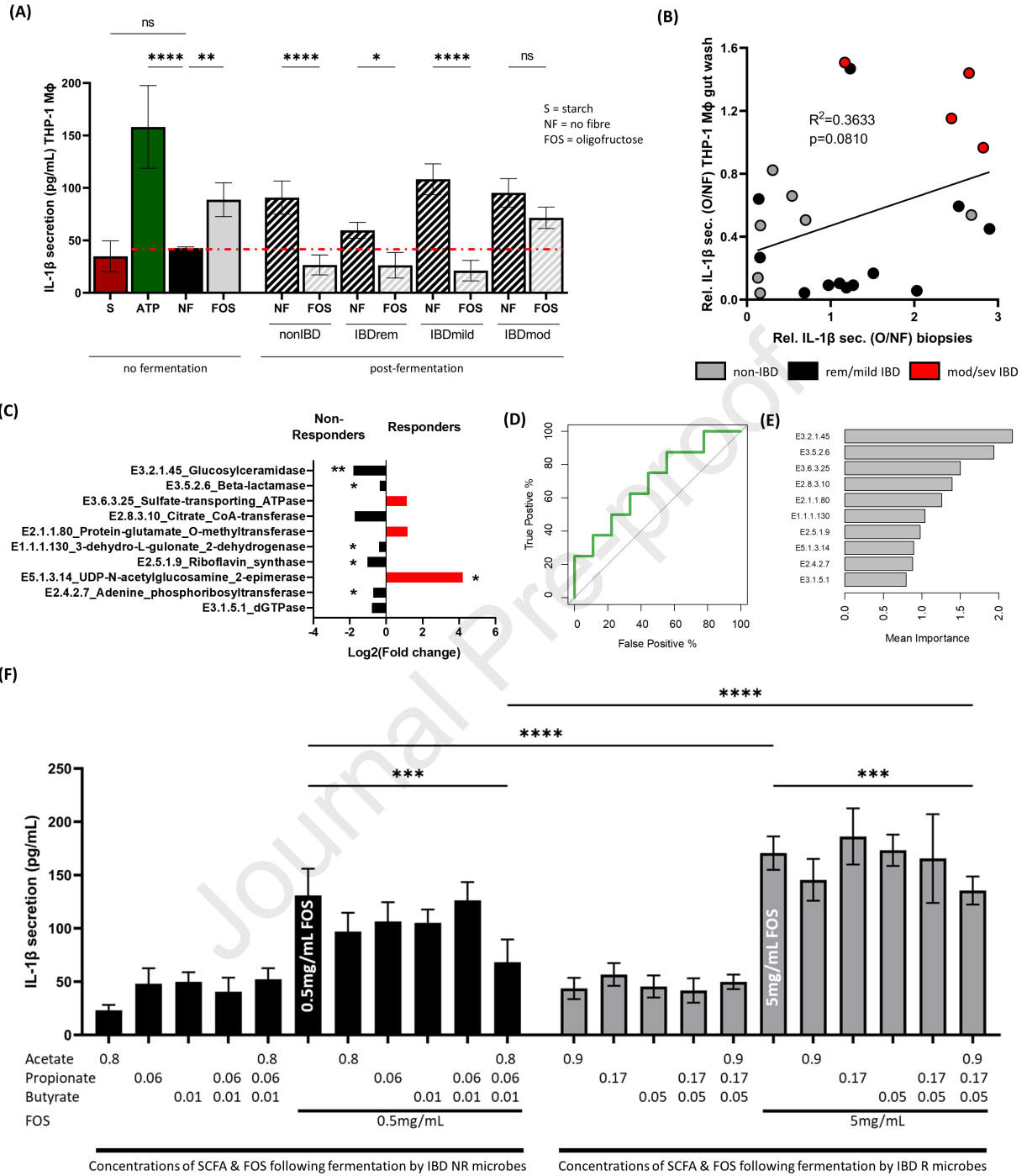
Armstrong *et al.* 2022

42. Parada Venegas D, De la Fuente MK, Landskron G, et al. Short Chain Fatty Acids (SCFAs)-Mediated Gut Epithelial and Immune Regulation and Its Relevance for Inflammatory Bowel Diseases. *Front Immunol* 2019;10:277.
43. Bajaj JS, Hylemon PB, Ridlon JM, et al. Colonic mucosal microbiome differs from stool microbiome in cirrhosis and hepatic encephalopathy and is linked to cognition and inflammation. *Am J Physiol Gastrointest Liver Physiol* 2012;303:G675-85.

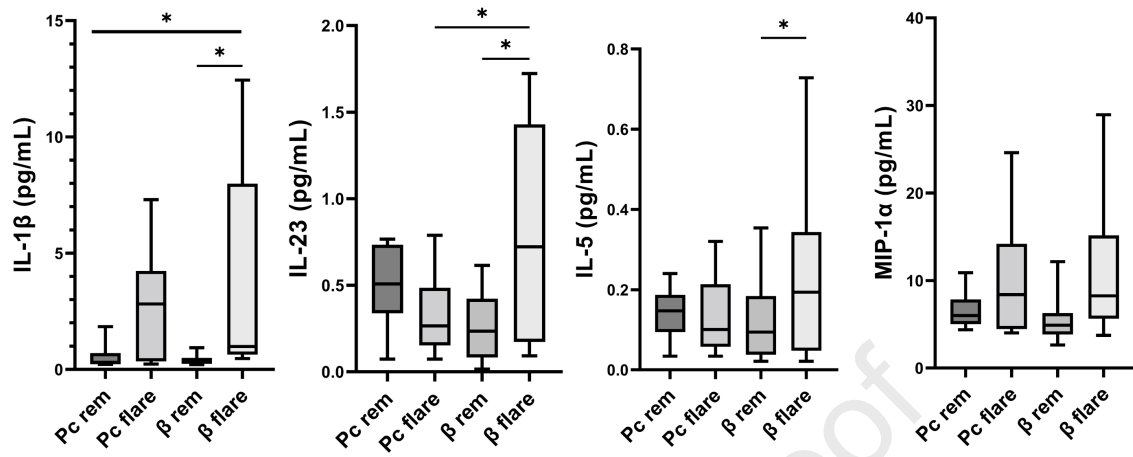
Journal Pre-proof



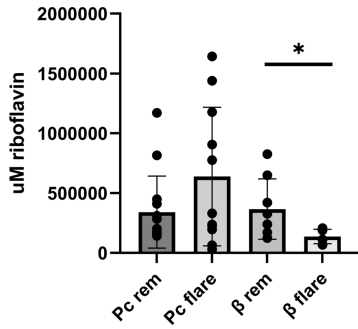




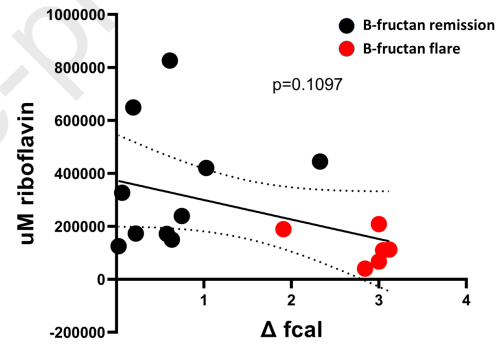
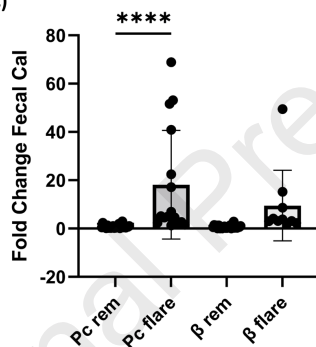
(A)



(B)



(C)



What You Need to Know

Background and Context

Inflammatory bowel diseases (IBD) are overall beneficially impacted by dietary fibers which are fermented by colonic microbes. Not all fibers are alike and patients report intolerance to fiber consumption.

New Findings

Unfermented dietary β -fructan fibers induced pro-inflammatory cytokines in a subset of IBD patient samples, via activation of the NLRP3 and TLR2 pathways; inflammation was reduced via fermentation by microbes.

Limitations

Fiber purity was confirmed yet microbial contaminants may be present. Mucosal microbes were collected, which are less impacted by bowel prep, however luminal microbiota are also important in fibre fermentation.

Clinical Research Relevance

Patients describe a sensitivity to dietary fibres however detrimental effects have been largely overlooked to date. Our data support further clinical investigations of the detrimental effects of specific dietary fibres and supports progression of personalized dietary fibre interventions designed to increase consumption of fibres that are safe for an individual, while avoiding detrimental fibres.

Basic Research Relevance

While fibers are typically beneficial in individuals with normal microbial fermentative potential, some dietary fibers have detrimental effects in select patients with active IBD who lack fermentative microbe activities. Here we show for the first time, unfermented β -fructan fibers induce inflammation via TLR2 and NLRP3 pathways.

Lay Summary

Dietary β -fructan fibers, if not effectively fermented by gut microbes, induce an inflammatory response and gut barrier changes in inflammatory bowel disease patients via TLR2 and activation of NLRP3

Journal Pre-proof

Armstrong *et al.* 2022

List of Supplementary materials:

Materials and Methods

Supplementary references

Table 1-6

Fig S1-S7

Journal Pre-proof

Materials and Methods**Key Resources Table**

REAGENT or RESOURCE	SOURCE	IDENTIFIER
Antibodies		
Zombie Aqua	BioLegend	423101
CD123	BioLegend	306018
CD3	BioLegend	317324
CD19	BioLegend	302246
CD11b	BioLegend	101230
CD16	BioLegend	302054
CD11c	eBioscience	35-0116-42
CD68	BioLegend	333816
CD14	BioLegend	301854
CD45	BioLegend	368514
Chemicals		
Protease inhibitor	Sigma Aldrich	P8340
Paraformaldehyde	Alfa Aesar	A11313
TRIzol	Ambion	15596018
HBSS	Gibco	14170-112
RPMI	Gibco	11875-093
FBS	Sigma Aldrich	F1051
PMA	Sigma Aldrich	P8139
LPS	Sigma Aldrich	L3012
HEPES	Gibco	15630-080
Penicillin/Streptomycin	Thermo Fisher	SV30010
DMEM/F12	Gibco	11330-032

Inulin HP	Beneo Orafti	Orafti HP
Inulin Sigma	Sigma Aldrich	9005-80-5
Oligofructose (FOS)	Beneo Orafti	Orafti P-95
Maltodextrin	Sigma Aldrich	419672
Zymosan A from <i>S. cerevisiae</i>	Sigma Aldrich	Z4250-250MG
Curdlan from <i>A. faecalis</i>	Sigma Aldrich	C7821-5G
Barley B-D-glucan	Sigma Aldrich	G6513
Fructose	Sigma Aldrich	F0127
Ac-YVAD-cmk	Sigma Aldrich	SML0429-1MG
Glyburide	Sigma Aldrich	G2539-5G
MCC905	InvivoGen	inh-mcc
TL2-c29	InvivoGen	inh-c29
BSA	Fisher Scientific	BP1600-100
SuperFrost-plus slides	Fisher Scientific	12-550-15
Goat serum	Invitrogen	50062Z
Dispase	Roche	04942078001
Collagenase P	Roche	C2139
DNase I	Invitrogen	LS18068015
Superscript IV VILO	Thermo Fisher	11756500
Power SYBR green	Thermo Fisher	4368702
Stabilwax-DA silica column	Restek Corp.	11040
Transwell	Corning	C3460
Critical Commercial Assays		
IL-1 β ELISA	R&D Systems	DY201-05
Mesoscale Discovery U-PLEX	Mesoscale Discovery	custom
microRNA prep kit	Cedarlane	R2060

Armstrong *et al.* 2022

Human chemokine PCR array	Origene	HPP6004C
RT ² qPCR profiler	Qiagen	330231
Fructose assay kit	Abcam	ab83380
QIAamp DNA Stool Mini Kit	Qiagen	51604
dsDNA High Sensitivity Assay	Agilent	5067-4627
Nextra XT DNA Preparation kit	Illumina Inc.	15032354
Deposited Data		
Metagenomics	This paper	
Experimental Models: Cell types		
Cell line: THP-1	ATCC	
Cell line: T84	ATCC	
PBMCs	Healthy participant blood	
Software and Algorithms		
CFX Manager Software V 3.0	Bio-Rad Laboratories, Inc.	
GraphPad Prism 4.0	GraphPad Software	
Kraken 2		
HUMAnN2		
Stata 14	StataCorp LLC	
ImageJ		
RandomForest R		

EXPERIMENTAL MODEL AND SUBJECT DETAILS

Consent and ethics approval

Consent was obtained from patients/guardians and assent from patients for collection of human samples; the study was approved by the University of Alberta Health Research Ethics Board (Study ID Pro00023820, Study ID Pro00046564 and Study ID Pro00092609), Edmonton, AB, Canada and the University of Manitoba (Study ID HS25294 and Study ID HS25252). All blood donors gave written informed consent in accordance with the Declaration of Helsinki.

Results were confirmed in biopsies and stool samples from our published single-center, double-blind, randomized, parallel, placebo controlled clinical trial (RCT), comparing the effectiveness of β -fructans (Synergy-1/Prebiotin; combination of oligofructose and inulin) versus maltodextrin (placebo).¹² All research procedures performed in this trial were in strict accordance with a predefined protocol and adherence to international GCP guidelines and Declaration of Helsinki. The research protocol was approved by Health Research Ethics Board (Study ID Pro00041938) at the University of Alberta and Natural Health Directorate at Health Canada. The study is publicly accessible at the U.S. National Institute of Health database (clinicaltrials.gov identification number NCT02865707). Deidentified samples were examined; fecal calprotectin measurements were provided as previously measured. Full details on patients and samples are provided in a separate publication.¹²

Pediatric IBD patient criteria and sample collection

Those eligible to participate consisted of patients aged 3–18 years, with histological and endoscopic confirmed diagnosis of CD or UC, based on the revised Porto criteria⁴⁴ and classified using the Paris classifications (or non-IBD controls).⁴⁵ We intentionally included patients with known disease (active or in remission) and new diagnoses to allow for a variety of biological scenarios. This study also included non-IBD control patients who underwent colonoscopy for abdominal pain and/or diarrhea suspected to have IBD, but endoscopy and histology were confirmed to be completely normal (most of the individuals were eventually diagnosed with functional abdominal disorders; completely healthy controls would have been ideal, but it would be unethical to expose them to an invasive procedure). Detailed inclusion and exclusion criteria were described previously.^{46, 47} Clinical details of patients included in the study were collected by chart review (**Table S5**). All patients participating in the study were on clear fluid diet for 24 hr and underwent standardized bowel cleansing prior to colonoscopy using Picosalax® (contains sodium picosulfate, magnesium oxide, and citric acid) prior to endoscopy. Procedures were performed under general anaesthesia (provided by a pediatric anaesthesiologist) using Propofol and Fentanyl.

Sample collection scheme is illustrated in **Fig. S1**. Aspirate washes and brushings from the terminal ileum (TI) were collected from patients during endoscopy, prior to collection of biopsies, at the Stollery Children's Hospital, University of Alberta in Edmonton, Alberta, Canada. Protease inhibitor (1% v:v; Sigma Aldrich) was added immediately to the aspirate washes, and further purified by filtration (40 μ m filters) and centrifugation at 200 g (5 min, 4°C) to discard food particles and human cells. The pellets containing bacteria were washed thrice in PBS (14000 g, 5 min, 4°C) and fixed in 4% (v:v) paraformaldehyde for 1 h, then washed and stored in 0.2% (w:v) BSA/PBS. The supernatants of bacterial intestinal washes were stored at -80°C for gas chromatography analysis and cell culture incubations. Mucosal brushings were stored in 1 mL trizol at -80°C prior to processing. Biopsy tissues were either fixed using an automated fixation system and paraffin embedded for immunohistochemistry, or were maintained in 20 mL of 100% HBSS on ice and immediately transported to the laboratory for *ex vivo* culturing. Clinical details of patients included in the study were collected, in accordance with the informed consent, by chart review (demographics, disease course, comorbidities, and current treatments), along with a Geboes histological score, as determined by blinded pathology scores performed by a clinical pathologist with a major interest in gastrointestinal pathology (Dr. Consolato Maria Sergi; **Table S5**).⁴⁸

Cell lines and reagents

Armstrong *et al.* 2022

The human monocyte cell line, THP-1, was obtained from the American Type Culture Collection (ATCC; Maryland, United States) and incubated (37°C, 5% CO₂) until confluent. THP-1 monocyte cells were maintained in RPMI-1640 supplemented with 10% Fetal Bovine Serum (FBS). Differentiation of THP-1 cells to macrophage lineage was performed using 25 nM phorbol 12-myristate 13-acetate (PMA; 48 hr followed by 24 hr rest) and subsequent stimulation with 10 ng/mL LPS for 3 hr prior to experimental treatment with fibers as indicated.⁴⁹

Human intestinal epithelial T84 cells (ATCC) were grown in DMEM/F12 media supplemented with 10% FBS and 100 units/mL of penicillin and 100 ug/ml streptomycin sulfate (37°C, 5% CO₂).

For all experimental settings, cultures were treated with 250 µl of oligofructose (5 mg/mL; Orafti P-95), inulin (5 mg/mL; Orafti HP), inulin (5 mg/mL; Sigma Aldrich), maltodextrin (5 mg/mL), β-D-glucan barley (1 g/L; Sigma-Aldrich), zymosan (100µg/mL; Sigma Aldrich), curdlin (100µg/mL; Sigma Aldrich), or fructose (Sigma Aldrich) as indicated, representing physiologically relevant concentrations; all treatments were confirmed to be LPS and endotoxin-free by ELISA. All fiber solutions were prepared in PBS and 5% culture media to provide nutrient to cell cultures. THP-1 macrophages were treated for 3 hr in 250 µl of fiber, as indicated. Biopsies cultured *ex vivo* and primary blood cultures were treated for 24 hr in 250 µl of fiber.

Isolation of human peripheral blood mononuclear cells (PBMCs)

PBMCs were isolated from nonIBD individuals with Lymphoprep™ Density Gradient Medium (STEMCELL Technologies) and cryopreserved in liquid nitrogen until thawed for fiber stimulation experiments. PBMCs were cultured (1.2million/ml) with or without FOS (5 mg/ml), maltodextrin (5 mg/ml) or zymosan (10 ug/ml) for 24 hrs in RPMI-1640 containing: 10% FBS, 100 U/mL Penicillin, 100 g/ml Streptomycin, 10 mM HEPES and 2 mM Glutamax (all from Thermofisher). In experiments with inhibitors, an inhibitor was added for 1hr (37°C, 5% CO₂) before addition of stimuli (MCC950, 1 uM, TL2-C29, 75 uM). Cell free supernatants were stored at -80°C until ELISA/Mesoscale Discovery assays.

Inhibition of NLRP3 inflammasome and TLR2 pathways

Differentiation of THP-1 cells to macrophage lineage was performed using 25 nM phorbol 12-myristate 13-acetate (PMA; 48 hr followed by 24 hr rest) and subsequent stimulation with YVAD (50 uM), Glyburide (200 uM), MCC950 (1uM), or TL2-C29 (75 uM) for 1 hr. Culture media was then replaced with a combination of indicated fiber plus inhibitor at previously mentioned concentrations for 24 hr and cell secretions were collected for ELISA or MSD.

Ex vivo culture of patient biopsy tissues

Biopsy tissues were collected from the terminal ileum and ascending colon (no significant differences in sample response were noted between locations in our particular experiments) during colonoscopy of pediatric IBD patients and non-IBD control patients, placed in cold HBSS, and transported on ice to the laboratory immediately. A core biopsy of tissue was dissected into 1-mm³ pieces and cultured in duplicate using a modified method as previously described.^{50, 51} Although not as physiologically ideal as directly treating patients with dietary factors, the *ex vivo* model provides advantages by measuring response of live human biopsies (containing all of the cell types within human intestinal tissues) to treatments in a more controlled environment (*e.g.*, devoid of wide variability in patient diets that may interfere with results analysis). Tissues were cultured on a presoaked gelatin sponge (Surgifoam) in 48-

Armstrong *et al.* 2022

well culture plates containing 250 μ L solution (PBS + indicated fiber, or PBS control; 5% DMEM/F12 [with 5% FBS], 100 U/mL penicillin/100 μ g/mL streptomycin antibiotic/antimycotic solution). Tissues were cultured in 250 μ L fiber or no fiber at 37°C for 24 hrs. Supernatants were collected for ELISA assays and remaining tissues were transferred to lysing matrix D bead beat tubes (MPbio) with 500 μ L TRIzol and stored at -80°C for RNA isolation.

ELISA

Supernatants were collected following treatment of cell lines or biopsy tissues with fiber or controls, as indicated. Supernatants were centrifuged at 14000g for 10 min to remove any cells or debris. Secreted IL-1 β was measured using an ELISA following manufacturers protocol (R&D Systems). Absorbance was measured by plate reader at 450 nm - 540 nm correction and calculations were performed using GraphPad Prism.

Flow Cytometry

Cells from pediatric patient biopsy tissues, collected during colonoscopy, were prepared for flow cytometry analysis following an altered method, as described by Fletcher *et al.* 2011.⁵² Briefly, biopsies were immediately placed in 10 mL of HBSS media for transport to the laboratory on ice. Media was removed and biopsies were placed in 2 mL of fresh enzyme mixture (RPMI-1640, 0.8 mg/ml Dispase [Roche], 0.2 mg/ml Collagenase P [Roche], 0.1 mg/ml DNase I [Invitrogen]) then incubated for 20 min in a 37 °C water bath. Biopsies were gently aspirated, 2 mL of enzyme media was replaced, and biopsies were disrupted using a 1mL pipet to release cells. Large fragments were allowed to settle for 30s; enzyme solution was moved to a tube containing 10 mL of ice-cold FACS buffer (2% FCS, 5 mM EDTA in PBS), 2 mL enzyme mix was re-added to remaining biopsy fragments, incubated in a 37 °C water bath for 5 min, and disrupted using a 1mL pipet to release cells. This step was repeated to a maximum of 50 min until no biopsy fragments remained. Cell mixtures were assessed for viability using trypan blue (viability exceeded 95%), then solutions were centrifuged (300 g, 4 min, 4°C), and pelleted cells were fixed in 4% formaldehyde for 10 min.

Samples were washed twice in PBS to remove fixative and resuspended in PBS + 10% FBS and incubated for 10 minutes at room temperature. Cells were then spun down and resuspended in flow buffer (PBS + 2 % FBS) containing diluted antibodies. Cells were then incubated in the dark for 30 minutes at 4°C, washed twice with flow buffer, resuspended in 200 μ L, and acquired on an Attune NxT flow cytometer (BVRY configuration, ThermoFisher Scientific). For each sample, the entire volume was acquired and analyzed, ranging from 4,000 - 400,000 events/sample. Data analysis was completed using FlowJo v 9 (BD Biosciences). Cells were gated based on FSC/SSC profiles to remove debris. Single cells were then gated based on FSC-A vs FSC-H. These cells were then gated for CD45 to exclude any non-immune cells. From here, cell populations were analyzed based on: T cells (CD45+, CD3+, CD19-), B cells (CD45+, CD3-, CD19+), Monocytes (CD45+, CD14+, CD16-), Neutrophils (CD45+, CD14-, CD16+), Macrophages (CD45+, CD68+), pDC (CD45+, CD123+, CD11c-), and cDC (CD45+, CD123-, CD11c+). All gate boundaries were set using FMO controls.

Fructose assay

Concentration of fructose in unfermented dietary fiber solutions was determined by fructose assay kit, following the manufacturer's directions (Abcam). To account for glucose interference, a series of fiber control solutions were prepared, which did not have the fructose converting enzyme added.

RNA isolation and gene expression analysis

Human cell lines and biopsy tissues were cultured as indicated and demonstrated in **Fig. S1**. RNA was isolated using TRIzol as previously described.⁵³ For human biopsy tissues, biopsies were first placed in lysing matrix D bead beat tubes (MPbio) with 500ul TRIzol (Thermo Fisher; MP116913050) and were bead beat for 2 x 40 s in the MP Biomedical Fastprep-24™ with 5 min on ice between cycles. For cell line experiments this step was not necessary and 1mL TRIzol lysates proceeded immediately to RNA extraction using Direct-zol microRNA prep kit (Zymo Research) following manufacturer's directions, including on column DNase I digestion. RNA was eluted using DNase/RNase free water, and cDNA libraries were prepared using Superscript IV VILO Mastermix (Thermo Fisher). POWER SYBR green PCR mastermix (Thermo Fisher) was used in RT-qPCR.

Origene human chemokines RTqPCR primer panel array plates (CAT#: HPP6004C) were used on human biopsies cultured *ex vivo* with NF or FOS (5 g/L) and QIAGEN RT² human inflammatory cytokines and receptors profiler (CAT#: 330231) was run on human cell lines (n=2) according to manufacturer's instructions. RT-qPCR was performed as previously described⁵³ to validate findings using the primers highlighted in **Table S6**. Both biological and technical replicates were performed on all reactions using housekeeping genes (GUSB and GAPDH). Data were analysed using CFX Manager Software Version 3.0 (Bio-Rad Laboratories, Inc.). Statistical significance was evaluated by the Wilcoxon unpaired *t*-test with Welch's correction using GraphPad Prism 9.0 (GraphPad Software, La Jolla, USA). RT-qPCR of targets of interest was performed to validate findings in non-IBD (n=12), CD (n=16), and UC (n=7) patient biopsies. RT-qPCR was further utilized to examine presence of CD45 in intestinal mucosal brushings (n=4).

Trans-Epithelial Electrical Resistance

T84 intestinal epithelial cells were seeded on the apical side of a 12mm, 0.4 μm transwell (Corning) at a density of 3.5×10^5 per well. The next day, maltodextrin (5 g/L), inulin HP (5 m/L), inulin Sigma (5 g/L), oligofructose (5 g/L), β-glucan (1 g/L), or NF control were added to the apical wells and the trans epithelial electrical resistance (TEER) was measured every day using a Millicell ERS voltohmmeter together with a STX1 electrode from World Precision Instruments (WPI). The fiber containing media was replaced every two days.

MesoScale Discovery (MSD) Multiplex ELISA

Protein secretions from pediatric patient *ex vivo* biopsies, and from adult UC patient biopsy tissue protein isolates, collected during colonoscopy visit were examined by MSD. Secreted proteins were collected following *ex vivo* culture and stored at -80°C. Protein extraction of adult UC biopsies was performed by adding biopsy tissues to Lysing Matrix D bead tubes (MPbio) along with 400μl NP-40 lysis buffer (1% NP-40, 150mM NaCl, 50mM Tris, pH 8.0). Tubes were bead beat for 40 seconds using MPBio FastPrep24. Total protein of samples was calculated by Bradford assay and samples were diluted to match the concentration of the most dilute protein sample. Secreted cytokines (IL-1β, IL-23, IL-5, MIP-1α) were measured following manufacturers protocol (MSD U-PLEX). Sample or standard was added to

Armstrong *et al.* 2022

the wells in duplicate. Absorbance was measured by MSD plate reader and calculated using Discovery Workbench 4.0 for Windows 10.

Molecular Docking of β -fructan (represented by Kestose-1) to TLR2 Heterodimers

We used two crystal structures containing TLR2 heterodimers for docking: TLR1-TLR2 (PDB ID: 2Z7X²⁸) and TLR2-TLR6 (PDB ID: 3A79²⁹). First, molecular dynamics (MD) simulations were carried out on these heterodimers. The simulations were used to provide an ensemble of conformations in solution in order to account for target flexibility.⁵⁴

All MD simulations were performed using GROMACS 2021.4^{55, 56} with the CHARMM36m force field⁵⁷ and the CHARMM-modified TIP3P water model.⁵⁸ Three replicate systems were simulated for each heterodimer (both TLR1-TLR2 and TLR2-TLR6). CHARMM-GUI⁵⁹ was used to add missing atoms and remove all non-protein molecules, such as ligands and carbohydrates. A rhombic dodecahedral box was constructed with a box edge distance of 10 Å from the nearest protein atom. Periodic boundary conditions were used. The simulation systems were neutralized by adding ions and solvated with water molecules; the TLR1-TLR2 system required 4 sodium ions and the TLR2-TLR6 system required 5 chloride ions. The total number of atoms was 225,286 and 246,363 for the TLR1-TLR2 and TLR2-TLR6 systems, respectively. A timestep of 2 fs was used. The LINCS algorithm⁶⁰ was used to constrain the lengths of bonds involving hydrogen atoms. Short-range electrostatic and Van der Waals interactions were calculated with a 9.5 Å cut-off. Long-range electrostatic interactions were calculated using PME-summation⁶¹ with fourth-order interpolation and a grid spacing of 1.2 Å. The Verlet cut-off scheme was used for neighbor searching. System equilibration was performed as follows. Energy minimization was performed using the steepest descent algorithm. The velocity rescaling thermostat⁶² was used to maintain the temperature in all of the simulations. A position restrained simulation with a force constant of 1000 kJ/mol was applied to heavy atoms in the NVT ensemble at 298 K for 1 ns. A subsequent 1 ns NPT simulation was performed using the Berendsen barostat.⁶³ Finally, a 1 ns NPT simulation using the Parrinello-Rahman barostat⁶⁴ completed the equilibration of the TLR2 heterodimer systems. For each system, three 100 ns production simulations were run in the NPT ensemble using the Parrinello-Rahman barostat.⁶⁴ Ten conformations were sampled from the last 60 ns from each of the three production simulations to obtain the TLR2 heterodimer conformations for docking.

Although AutoDock-GPU⁶⁵ allows some bonds in the ligand to be rotatable, bonds in cyclic groups are not rotatable. This provided the motivation to use MD simulations to obtain additional conformational sampling for kestose-1. A 600 ns simulation of kestose-1 was performed to obtain heterogeneous conformations of the ligand for docking. The structure of kestose-1 was constructed using ChimeraX.⁶⁶ Kestose-1 parameters were generated using CGenFF.⁶⁷⁻⁶⁹ All simulation parameters were the same as those used in the TLR2 heterodimer simulations (see above). Energy minimization was performed using the steepest descent algorithm, followed by a 600 ns NVT production simulation. Thirty different kestose-1 conformations were generated by taking conformations every 10 ns from the last 300 ns of the production simulation; these provide a unique kestose-1 conformation for each independent docking run.

AutoDock-GPU⁶⁵ was used to perform the docking pose prediction of kestose-1 onto the TLR2 heterodimer systems. A docking search of the entire protein dimer was conducted in a two-step process. First, kestose-1 was docked onto the entire dimer. Based on the locations of these predicted

poses, a comprehensive docking search was focussed on these specific regions. Details of this two-step process are outlined below.

The first step of our docking procedure was performed as follows. For each of the conformations provided by the TLR2 heterodimer simulations, multiple grid boxes were placed such that the search space encompassed the entire dimer. The size of each grid box was 75 Å × 75 Å × 75 Å, comprised of the default grid spacing of 0.375 Å and 200 grid points along the x, y, and z dimensions. Furthermore, the grid center for each of these grid boxes was positioned such that for any given grid box, there exists another grid box that overlaps with at least 25% of the volume of the given grid box. This was done to ensure that the search space did not include boundaries that had limited sampling. The default settings for AutoDock-GPU⁶⁵ were used with the following exceptions: 100 Lamarckian Genetic Algorithm⁷⁰ (LGA) runs, 8192000 score generations per LGA run, and 99999 generations per LGA run. Over 40,000 poses were generated for each heterodimer system.

The second step involves performing localized docking on the clusters of kestose-1 poses generated from the first step of docking. AutoDockTools⁷¹ was used to determine the root atom of the kestose-1 molecule, which was used as the grid box center. New grid boxes were generated, centered about the root atom in each of the top ~1 % of docked poses based on their predicted binding free energy. The size of each refined grid box was 30 Å × 30 Å × 30 Å, comprised of a smaller grid spacing of 0.150 Å and 200 grid points along the x, y, and z dimensions.

Many of these grid boxes were highly overlapped since many of the predicted poses were closely clustered. We developed an algorithm to reduce the number of grid boxes required. First, we start by selecting the grid box that encloses the greatest number of predicted poses. This selected grid box is stored, and the poses contained within it are removed from the set of predicted poses. Next, we select the grid box that encloses the greatest number of poses from the remaining poses. We repeat this cycle until all poses are accounted for. The selected grid boxes are then used for the next step of docking. Again, the default settings for AutoDock-GPU⁶⁵ were used with the following exceptions: 100 LGA runs, 8192000 score generations per LGA run, and 99999 generations per LGA run.⁷⁰ The best kestose-1 poses were selected from this final pool of predicted poses based on their binding free energy. VMD was used for all molecular visualization.⁷²

Anaerobic culture of patient intestinal washes

Whole microbiome liquid cultures (intestinal washes) were obtained during colonoscopy by directing 30 mL of sterile normal saline against the mucosal wall of the intestine in uninflamed areas of the terminal ileum or ascending colon (no significant difference between sample locations was noted in our findings) and then collecting the fluid into a container using the endoscope suction system.⁷³ Samples were transported on ice to the laboratory under 30 min post collection. Live microbe cultures were immediately isolated by centrifugation and moved to the anaerobic chamber. Culture density was measured on a spectrophotometer and cultures were back-diluted to an OD₆₀₀ of 1.0 and split into two equal samples. Microbe pellets were collected and resuspended in 10mL of NF or oligofructose (5 mg/mL) solution, supplemented with 5% BHI media, and cultured anaerobically at 37°C. Whole microbe cultures were allowed to ferment NF or oligofructose for 24 hr. At this time point we observed no significant changes in microbe abundance (shotgun metagenomics) and we had confirmed that fiber fermentation (HPLC) and SCFA production (GC:VFA) occurred. Microbes were then centrifuged out of culture for 10 min at 3500 rpm. Microbe isolates were prepared for shotgun metagenomic sequencing,

while supernatants were isolated to create fermentation by-product supernatant solutions (post-fermentation solution) for SCFA measurement or further incubation with THP-1 macrophage cells. 1 mL of each post-fermentation solution was sent for volatile fatty acid (VFA) analysis, while the remainder of culture was used to treat macrophage cells to determine the ability of patient whole microbe cultures to ferment oligofructose and reduce secretion of pro-inflammatory cytokines.

Gas chromatography for volatile fatty acids

The concentrations of SCFA in intestinal wash supernatants were determined using VFA analysis by gas chromatography performed by Department of Agriculture, chromatography core at the University of Alberta. Intestinal washes were collected during colonoscopy, incubated with fiber, supernatants were centrifugation (3000 xg for 10 min), as described above, and samples were stored at -80°C for VFA analysis.

Samples were thawed and prepared just before use by adding 200 µL of 25% phosphoric acid and centrifuging for 15 minutes at 13,000 rpm. Then 1 mL of supernatant was combined with 200 µL of the internal standard in a GC vial for analysis. Isocaproic acid was used as internal standard. Samples were run on a Varian 430-GC with FID (Varian, Inc., USA) using a Stabilwax-DA fused silica column (Restek Corp., 30 meter, 0.53 mm ID, 0.5 µm film). The carrier gas was helium at 10 ml/min. The injector and detector temperatures were maintained at 250°C, and the injection split was 5:1. The injection volume was 1 µL. The oven was held for 0 min at 80°C, then increased to 180°C at 20°C/min and held for 3 min for a total run time of 8 min. Retention times and concentrations were determined using standard compounds and the internal standard. SCFA production in these anaerobic cultures was similar to patterns observed in previously published studies of IBD examining stool and luminal content in patients.⁷

NGS library construction and shotgun metagenomics

Library construction and sequencing

Genomic DNA from aspirate washes was extracted using the QIAamp DNA Stool Mini Kit (Qiagen, Mississauga, ON, Canada) with additional steps to assure bacterial cell lysis of Gram-positive bacteria. Briefly, samples were washed in 1 ml of TN150 buffer (10 mM Tris-HCl, 150 mM NaCl [pH 8.0]), followed by incubation with SDS (10 % w/v) and proteinase K (20 mg /mL) at 55°C for 2h. Cells were then physically disrupted with zirconium beads (diameter 0.1 mm; 300 mg) in a FastPrep-24 (MP Biomedicals, Solon, OH) in 3 cycles of 30-second bead-beating step at 4 m/s speed followed by cooling on ice for 5 min each. Subsequently, samples were heated at 95°C for 15 min and further processed according to the kit protocol. DNA was then quantified using a Qubit 2.0 Fluorometer with the dsDNA HighSensitivity Assay quantification kit (ThermoFisher). Libraries were constructed from 1 ng of DNA using the Nextera XT DNA Preparation Kit (Illumina Inc.). Briefly, the genomic DNA was incubated with the transposome to perform a tagmentation reaction, which fragmented the DNA and added adapter sequences at the 5' and 3' ends of each amplicon. The products were then amplified by 12 cycles of PCR using specific index adapters for Illumina sequencing (Nextera XT Index Kit v2, Illumina). The resulting libraries were cleaned up using AMPure beads (bead:library at 1.8:1 ratio), eluted in 50 µl of kit resuspension buffer, and

Armstrong *et al.* 2022

quantified on Qubit 2.0 Fluorometer. The cleaned libraries were then re-amplified using the same index adapters as some of the samples yielded low concentration (<1 ng/ μ L). All libraries were then assayed on QIAxcel Fragment Analyzer System (Agilent) to identify average library size and further quantified using Qubit Fluorometer prior to sequencing to calculate molarity. Multiplexed libraries were sequenced on a NovaSeq 6000 system (Illumina Inc.) using a S2 flow cell at an average depth of 100 million reads per sample.

Bioinformatics analysis

Sequences were inspected with Fastqc (<https://www.bioinformatics.babraham.ac.uk/projects/fastqc/>) and bases at the end of reads with quality scores (Qscore) smaller than 30 were trimmed with mcf-fastq (<https://github.com/ExpressionAnalysis/ea-utils/blob/wiki/FastqMcf.md>), allowing a minimal length of trimmed reads of 120 base pairs. Taxonomic classification was conducted with Kraken2⁷⁴ and a customized database was compiled using the standard Kraken2 database, supplemented with bacterial genomes in the Genome Taxonomy Database (GTDB; gtdb.ecogenomic.org). The GTDB hosts 145,512 bacterial accessions and 2,392 archaeal accession.⁷⁴ Kraken2 hits accumulating less than 10% of K-mers matching the reference sequence were discarded and a hit was considered true only if at least 50 reads were aligned against the reference. For metabolic profiling, HUMAnN2⁷⁵ was used. Output tables were labelled with UniRef90 names using the script `human2_rename_table`, and gene family abundance was renormalized with script `humann2_renorm_table`, from RPK to compositional units (counts per million) to enable between-sample comparisons. Genes were regrouped to functional categories with script `humann2_regroup_table`, to enzyme commission (EC) categories level 4.

Metabolomics

Metabolites were isolated from patient stool samples as directed by the Calgary Metabolomics Research Facility, University of Calgary. On ice, 100-200mg of stool were measured into 1.5mL Eppendorf tubes and weights were recorded. Five volumes of pre-chilled methanol was added to each sample, then homogenized at max speed in the MPBio Fastprep24 bead beater for 1 min. Samples were incubated on ice for 30min then centrifuged at max speed, 4°C, for 10min. Supernatants were gently removed so as not to disrupt the pellet. Supernatants were processed for μ M concentration of riboflavin by Calgary Metabolomics Research Facility staff.

Food frequency questionnaire

A semi-quantitative food frequency questionnaire (FFQ), previously validated for use in Canadian pediatric and adolescent populations,⁷⁶ was utilized to collect dietary intake patterns, reflecting the previous 12 months. FFQs were considered valid if completed within 90 days of specimen collection; for younger children, parents completed the FFQs. To provide an updated reflection of caloric values, and as the original FFQ analysis software was no longer available and current for use, the Canadian Nutrient File (CNF) online database (Health Canada, 2015. <https://food-nutrition.canada.ca/>) was used to

generate an estimated caloric value for each FFQ item, obtained by averaging three similar items from the CNF. Calories for items were adjusted to include modifications of items such as frying, using extra-lean meats or low-calorie or reduced-fat options. Respondents reported if serving sizes were larger than, smaller than, or approximately equal to the given example portion size, and caloric values were adjusted accordingly. Estimated daily kilocalorie values were calculated for each patient and verified for plausibility against patient age and weight. A fiber content database of fiber subtype for each FFQ item was generated utilizing published data on food fiber contents.⁷⁷⁻⁸⁹ This fiber database was used to calculate approximate daily intakes of each of four fiber subtypes: inulin, oligofructose, pectin, and β -glucan, based on the FFQ entries. Fiber intake estimates were then kilocalorie-adjusted using the Willett residuals method as described by Willett *et al*⁹⁰ using Stata 14.⁹¹ Spearman correlation with fiber content was analyzed in Stata 14⁹¹ for correlations with intestinal wash SCFA content and proportions, as well as fold change in biopsy IL-1 β production in response to oligofructose exposure.

QUANTIFICATION AND STATISTICAL ANALYSIS

Shotgun metagenomics data analysis

Row sequencing reads were deposited at the Short Reads Archive (SRA) database of NCBI and are publicly available under accession number PRJNA690735.

To identify potential determinants of host-microbiota interactions that are predictive of response to oligofructose, separate random forest classifiers (RFCs) were independently trained on changes in fecal microbial composition and enzymes using the randomForest package in R.⁹² Area under the receiver operating characteristic curves (AUC-ROCs) were then used to evaluate RFC performance, where AUC-ROCs ≥ 0.70 were considered acceptable accuracy.⁹³ Mann Whitney U test were performed between the response to oligofructose and its best predictors, where p values < 0.05 were considered significant.

Statistical Analysis

In addition to specific statistical methods described in some of the sections above for individual analyses, groups were compared using paired Wilcoxon *t*-test (two-tailed) analysis, ANOVA, or Kendall, depending on the relevant question, using Microsoft Excel and GraphPad Prism. Spearman correlations were performed using Stata 14. A P value of < 0.05 was considered as significant in all cases, unless indicated, and all error deviations are described by \pm SEM. Measurements were completed using a minimum of two technical replicates and 3 biological replicates for all experiments.

Supplementary References

44. Levine A, Koletzko S, Turner D, et al. ESPGHAN revised porto criteria for the diagnosis of inflammatory bowel disease in children and adolescents. *J Pediatr Gastroenterol Nutr* 2014;58:795-806.
45. Levine A, Griffiths A, Markowitz J, et al. Pediatric modification of the Montreal classification for inflammatory bowel disease: the Paris classification. *Inflamm Bowel Dis* 2011;17:1314-21.

46. Zaidi D, Churchill L, Huynh HQ, et al. Capillary Flow Rates in the Duodenum of Pediatric Ulcerative Colitis Patients Are Increased and Unrelated to Inflammation. *J Pediatr Gastroenterol Nutr* 2017;65:306-310.
47. Alipour M, Zaidi D, Valcheva R, et al. Mucosal Barrier Depletion and Loss of Bacterial Diversity are Primary Abnormalities in Paediatric Ulcerative Colitis. *J Crohns Colitis* 2016;10:462-71.
48. Geboes K, Riddell R, Ost A, et al. A reproducible grading scale for histological assessment of inflammation in ulcerative colitis. *Gut* 2000;47:404-9.
49. Lund ME, To J, O'Brien BA, et al. The choice of phorbol 12-myristate 13-acetate differentiation protocol influences the response of THP-1 macrophages to a pro-inflammatory stimulus. *J Immunol Methods* 2016;430:64-70.
50. Armstrong HK, Gillis JL, Johnson IRD, et al. Dysregulated fibronectin trafficking by Hsp90 inhibition restricts prostate cancer cell invasion. *Sci Rep* 2018;8:2090.
51. Udden SM, Waliullah S, Harris M, et al. The Ex Vivo Colon Organ Culture and Its Use in Antimicrobial Host Defense Studies. *J Vis Exp* 2017.
52. Fletcher AL, Malhotra D, Acton SE, et al. Reproducible isolation of lymph node stromal cells reveals site-dependent differences in fibroblastic reticular cells. *Front Immunol* 2011;2:35.
53. Gillis JL, Selth LA, Centenera MM, et al. Constitutively-active androgen receptor variants function independently of the HSP90 chaperone but do not confer resistance to HSP90 inhibitors. *Oncotarget* 2013;4:691-704.
54. Santos LHS, Ferreira RS, Caffarena ER. Integrating Molecular Docking and Molecular Dynamics Simulations. *Methods Mol Biol* 2019;2053:13-34.
55. Mark James Abraham, Teemu Murtola, Roland Schulz, et al. GROMACS: High performance molecular simulations through multi-level parallelism from laptops to supercomputers. *SoftwareX* 2015;1-2:19-25.
56. Páll S, Abraham MJ, Kutzner C, et al. Tackling Exascale Software Challenges in Molecular Dynamics Simulations with GROMACS. Springer, Cham 2015.
57. Huang J, Rauscher S, Nawrocki G, et al. CHARMM36m: an improved force field for folded and intrinsically disordered proteins. *Nat Methods* 2017;14:71-73.
58. MacKerell AD, Bashford D, Bellott M, et al. All-atom empirical potential for molecular modeling and dynamics studies of proteins. *J Phys Chem B* 1998;102:3586-616.
59. Jo S, Kim T, Iyer VG, et al. CHARMM-GUI: a web-based graphical user interface for CHARMM. *J Comput Chem* 2008;29:1859-65.
60. Berk Hess, Henk Bekker, Herman J. C. Berendsen, et al. LINCS: A linear constraint solver for molecular simulations. *Journal of Computational Chemistry* 1998;18:1463-1472.
61. Essmann U, Perera L, Berkowitz ML, et al. A smooth particle mesh Ewald method. *The Journal of Chemical Physics* 1995;103:8577-8593.
62. Bussi G, Donadio D, Parrinello M. Canonical sampling through velocity rescaling. *J Chem Phys* 2007;126:014101.
63. Berendsen HJC, Postma JPM, Gunsteren WFV, et al. Molecular dynamics with coupling to an external bath. *The Journal of Chemical Physics* 1984;81:3684-3690.
64. Parrinello M, Rahman A. Polymorphic transitions in single crystals: A new molecular dynamics method. *Journal of Applied Physics* 1981;52:7182-7190.
65. Santos-Martins D, Solis-Vasquez L, Tillack AF, et al. Accelerating AutoDock4 with GPUs and Gradient-Based Local Search. *J Chem Theory Comput* 2021;17:1060-1073.
66. Pettersen EF, Goddard TD, Huang CC, et al. UCSF ChimeraX: Structure visualization for researchers, educators, and developers. *Protein Sci* 2021;30:70-82.
67. Vanommeslaeghe K, MacKerell AD, Jr. Automation of the CHARMM General Force Field (CGenFF) I: bond perception and atom typing. *J Chem Inf Model* 2012;52:3144-54.

68. Vanommeslaeghe K, Raman EP, MacKerell AD, Jr. Automation of the CHARMM General Force Field (CGenFF) II: assignment of bonded parameters and partial atomic charges. *J Chem Inf Model* 2012;52:3155-68.
69. Vanommeslaeghe K, Hatcher E, Acharya C, et al. CHARMM general force field: A force field for drug-like molecules compatible with the CHARMM all-atom additive biological force fields. *J Comput Chem* 2010;31:671-90.
70. Morris GM, Goodsell DS, Halliday RS, et al. Automated docking using a Lamarckian genetic algorithm and an empirical binding free energy function. *Journal of Computational Chemistry* 1998;19:1639-1662.
71. Morris GM, Huey R, Lindstrom W, et al. AutoDock4 and AutoDockTools4: Automated docking with selective receptor flexibility. *J Comput Chem* 2009;30:2785-91.
72. Humphrey W, Dalke A, Schulten K. VMD: visual molecular dynamics. *J Mol Graph* 1996;14:33-8, 27-8.
73. Zaidi D, Huynh HQ, Carroll MW, et al. Gut Microenvironment and Bacterial Invasion in Paediatric Inflammatory Bowel Diseases. *J Pediatr Gastroenterol Nutr* 2020;71:624-632.
74. Chaumeil PA, Mussig AJ, Hugenholtz P, et al. GTDB-Tk: a toolkit to classify genomes with the Genome Taxonomy Database. *Bioinformatics* 2019.
75. Franzosa EA, Mclver LJ, Rahnavaard G, et al. Species-level functional profiling of metagenomes and metatranscriptomes. *Nat Methods* 2018;15:962-968.
76. Shatenstein B, Amre D, Jabbour M, et al. Examining the relative validity of an adult food frequency questionnaire in children and adolescents. *Journal of pediatric gastroenterology and nutrition* 2010;51:645-652.
77. Stevenson L, Phillips F, O'sullivan K, et al. Wheat bran: its composition and benefits to health, a European perspective. *International journal of food sciences and nutrition* 2012;63:1001-1013.
78. Mei X, Mu T-H, Han J-J. Composition and physicochemical properties of dietary fiber extracted from residues of 10 varieties of sweet potato by a sieving method. *Journal of Agricultural and Food Chemistry* 2010;58:7305-7310.
79. Moshfegh AJ, Friday JE, Goldman JP, et al. Presence of inulin and oligofructose in the diets of Americans. *The Journal of nutrition* 1999;129:1407S-1411S.
80. Ross JK. Dietary fiber values for various breads are higher using enzymatic analysis rather than detergent analysis. *Journal of the American Dietetic Association* 1994;94:166-168.
81. Ranganna S, Govindarajan V, Ramana K, et al. Citrus fruits—Varieties, chemistry, technology, and quality evaluation. Part II. Chemistry, technology, and quality evaluation. *A. Chemistry. Critical Reviews in Food Science & Nutrition* 1983;18:313-386.
82. Fernando B. Rice as a Source of Fibre. *J Rice Res* 1: e101. doi: 10.4172/jrr. 1000e101 Page 2 of 4 Volume 1 • Issue 2 • 1000e101 *J Rice Res* ISSN: JRR, an open access journal Figure 3: Rice grain structure Source: Juliano [8]. Rice fraction Crude protein (g N x 5.95) Crude fat (g) Crude fibre (g) Crude ash (g) Available carbohydrates (g) Neutral detergent fibre (g) Energy content (kJ) Rough rice 2013:5.8-7.7.
83. de Almeida Costa GE, da Silva Queiroz-Monici K, Reis SMPM, et al. Chemical composition, dietary fibre and resistant starch contents of raw and cooked pea, common bean, chickpea and lentil legumes. *Food chemistry* 2006;94:327-330.
84. Li S, Zhu D, Li K, et al. Soybean curd residue: composition, utilization, and related limiting factors. *International Scholarly Research Notices* 2013;2013.
85. Saha BC, Dien BS, Bothast RJ. Fuel ethanol production from corn fiber current status and technical prospects. *Biotechnology for fuels and chemicals: Springer*, 1998:115-125.
86. Belorkar SA, Gupta A. Oligosaccharides: a boon from nature's desk. *Amb Express* 2016;6:82.

Armstrong *et al.* 2022

87. Van Buggenhout S, Sila D, Duvetter T, et al. Pectins in processed fruits and vegetables: Part III—Texture engineering. *Comprehensive Reviews in Food Science and Food Safety* 2009;8:105-117.
88. Jovanovic-Malinovska R, Kuzmanova S, Winkelhausen E. Oligosaccharide profile in fruits and vegetables as sources of prebiotics and functional foods. *International journal of food properties* 2014;17:949-965.
89. Baker RA. Reassessment of some fruit and vegetable pectin levels. *Journal of Food Science* 1997;62:225-229.
90. Willett WC, Howe GR, Kushi LH. Adjustment for total energy intake in epidemiologic studies. *The American journal of clinical nutrition* 1997;65:1220S-1228S.
91. StataCorp. *Stata Statistical Software: Release 14*. College Station, TX: StataCorp LLC, 2015.
92. Liaw A, Wiener M. Classification and Regression by randomForest. *R News* 2002;2.
93. Xia J, Broadhurst DI, Wilson M, et al. Translational biomarker discovery in clinical metabolomics: an introductory tutorial. *Metabolomics* 2013;9:280-299

Supplementary Table 1: Dietary carbohydrate chemical features

	Inulin HP	Inulin Sigma	FOS P95	B-D-glucan	β-1,3-glucan	Maltodextrin
Chemistry	Glu+Fru _n DP 10-60	Glu+Fru _n DP 2-60	Glu+Fru _n DP 2-8	Glu+Glu _n DP 2-5	Glu+Glu _n DP >62	Glu+Glu _n DP 3-9
DP_{avg}	25	12	4	3	>62	6
Content (% dry matter)	99.5	92	95	>95		
Sugars (% dry matter)	<0.5	8	5	<5		
H₂O Solubility (% at 25°C)	2.5	12	>75	>75	insoluble	100
Branching	linear	linear	linear	linear	branched	linear
Source	chicory	chicory	chicory	barley	fungi	corn

* Degree of polymerization or number of saccharide units (DP)

Supplementary Table 2: Shotgun metagenomic sequencing mean relative species abundance by patient diagnosis

Phylum	Species	Disease			SEM		
		Non-IBD	CD	UC	Non-IBD	CD	UC
Firmicutes	Faecalibacterium.s__Faecalibacterium_prausnitzii	25.85%	17.58%	24.93%	3.55%	3.59%	3.30%
Firmicutes	Flavonifractor.s__Flavonifractor_plautii	0.18%	2.48%	8.48%	0.06%	1.33%	2.15%
Firmicutes	Lachnospiraceae_noname.s__Lachnospiraceae_bacterium_7_1_58FAA	0.44%	2.54%	2.14%	0.15%	0.59%	0.63%
Firmicutes	Blautia.s__Ruminococcus_torques	2.35%	1.74%	1.67%	1.07%	0.58%	0.99%
Firmicutes	Blautia.s__Ruminococcus_gnavus	0.58%	1.08%	1.85%	0.21%	0.22%	0.09%
Firmicutes	Eubacterium.s__Eubacterium_rectale	2.25%	0.44%	0.45%	0.56%	0.23%	0.16%
Firmicutes	Clostridium.s__Clostridium_bolteae	0.54%	0.28%	0.16%	0.19%	0.25%	0.10%
Firmicutes	Roseburia.s__Roseburia_inulinivorans	0.70%	0.30%	0.32%	0.20%	0.23%	0.12%
Firmicutes	Coprococcus.s__Coprococcus_comes	0.27%	0.38%	0.43%	0.12%	0.23%	0.07%
Firmicutes	Lachnospiraceae_noname.s__Lachnospiraceae_bacterium_3_1_46FAA	0.21%	0.39%	0.57%	0.09%	0.29%	0.48%
Firmicutes	Dorea.s__Dorea_formicigenans	0.32%	0.32%	0.47%	0.15%	0.16%	0.15%
Firmicutes	Erysipelotrichaceae_noname.s__Clostridium_amosum	0.95%	0.17%	0.47%	0.42%	0.10%	0.00%
Firmicutes	Clostridium.s__Clostridium_clostridioforme	0.00%	0.25%	0.30%	0.00%	0.31%	0.19%
Firmicutes	Lachnospiraceae_noname.s__Lachnospiraceae_bacterium_5_1_63FAA	1.05%	0.08%	0.14%	0.43%	0.06%	0.04%
Firmicutes	Ruminococcus.s__Ruminococcus_lactaris	0.45%	0.31%	0.13%	0.23%	0.32%	0.16%
Firmicutes	Dorea.s__Dorea_longicatena	0.51%	0.25%	0.27%	0.18%	0.12%	0.03%
Firmicutes	Anaerostipes.s__Anaerostipes_hadrus	1.06%	0.09%	0.03%	0.42%	0.07%	0.00%
Firmicutes	Eubacterium.s__Eubacterium_hallii	0.36%	0.14%	0.15%	0.10%	0.09%	0.03%
Firmicutes	Roseburia.s__Roseburia_hominis	0.20%	0.14%	0.09%	0.14%	0.09%	0.12%
Firmicutes	Lachnospiraceae_noname.s__Lachnospiraceae_bacterium_2_1_58FAA	0.20%	0.19%	0.01%	0.09%	0.03%	0.00%
Firmicutes	Eubacterium.s__Eubacterium_sp_3_1_31	0.39%	0.11%	0.05%	0.13%	0.06%	0.04%
Firmicutes	Eubacterium.s__Eubacterium_ramulus	0.12%	0.02%	0.36%	0.08%	0.03%	0.04%
Firmicutes	Clostridium.s__Clostridium_hathewayi	0.32%	0.14%	0.00%	0.12%	0.17%	0.00%
Firmicutes	Holdemania.s__Holdemania_filiformis	0.07%	0.11%	0.07%	0.05%	0.09%	0.02%
Firmicutes	Clostridium.s__Clostridium_nexile	0.00%	0.01%	0.03%	0.00%	0.01%	0.04%
Firmicutes	Ruminococcus.s__Ruminococcus_bromii	0.00%	0.09%	0.19%	0.00%	0.07%	0.10%
Firmicutes	Lachnospiraceae_noname.s__Lachnospiraceae_bacterium_1_4_56FAA	0.08%	0.09%	0.01%	0.03%	0.01%	0.01%
Firmicutes	Coprococcus.s__Coprococcus_catus	0.20%	0.03%	0.10%	0.07%	0.03%	0.01%
Bacteroidetes	Alistipes.s__Alistipes_putredinis	3.41%	3.30%	4.19%	1.68%	1.33%	2.43%
Bacteroidetes	Bacteroides.s__Bacteroides_fragilis	2.15%	4.95%	1.09%	1.47%	1.54%	0.32%
Bacteroidetes	Bacteroides.s__Bacteroides_vulgatus	0.94%	4.21%	2.52%	0.64%	1.34%	0.34%
Bacteroidetes	Alistipes.s__Alistipes_ponderosus	0.92%	1.65%	0.60%	0.33%	0.68%	0.40%
Bacteroidetes	Bacteroides.s__Bacteroides_uniformis	2.64%	2.17%	1.60%	0.66%	0.63%	1.05%
Bacteroidetes	Bacteroides.s__Bacteroides_dorei	2.16%	1.63%	1.75%	0.91%	0.81%	1.65%
Bacteroidetes	Bacteroides.s__Bacteroides_caccae	2.78%	0.82%	1.39%	0.63%	0.49%	0.72%
Bacteroidetes	Bacteroides.s__Bacteroides_ovatus	0.90%	0.83%	0.71%	0.41%	0.59%	0.55%
Bacteroidetes	Bacteroides.s__Bacteroides_coprocola	4.12%	0.26%	0.00%	1.82%	0.10%	0.00%
Bacteroidetes	Blautia.s__Ruminococcus_obeum	1.72%	0.44%	1.05%	0.32%	0.26%	0.19%
Bacteroidetes	Bacteroides.s__Bacteroides_thetaiotaomicron	0.84%	0.53%	0.38%	0.22%	0.08%	0.21%
Bacteroidetes	Parabacteroides.s__Parabacteroides_merdae	1.26%	0.68%	0.35%	0.42%	0.40%	0.30%
Bacteroidetes	Parabacteroides.s__Parabacteroides_distasonis	2.00%	0.14%	0.37%	0.39%	0.04%	0.19%
Bacteroidetes	Alistipes.s__Alistipes_shahii	0.17%	0.35%	0.34%	0.08%	0.14%	0.11%
Bacteroidetes	Alistipes.s__Alistipes_finegoldii	0.00%	0.33%	0.01%	0.00%	0.22%	0.01%
Bacteroidetes	Prevotella.s__Prevotella_copri	0.73%	0.26%	0.51%	0.32%	0.33%	0.02%
Bacteroidetes	Bacteroides.s__Bacteroides_stercoris	1.27%	0.03%	0.17%	0.29%	0.02%	0.00%
Bacteroidetes	Bacteroides.s__Bacteroides_massiliensis	1.71%	0.00%	0.05%	0.67%	0.00%	0.06%
Bacteroidetes	Bacteroidales_noname.s__Bacteroidales_bacterium_ph8	0.45%	0.25%	0.00%	0.15%	0.25%	0.00%
Bacteroidetes	Barnesiella.s__Barnesiella_intestinihominis	0.35%	0.04%	0.24%	0.11%	0.05%	0.24%
Bacteroidetes	Bacteroides.s__Bacteroides_xylanisolvens	0.00%	0.15%	0.08%	0.00%	0.08%	0.00%
Bacteroidetes	Bacteroides.s__Bacteroides_plebeius	0.00%	0.04%	0.10%	0.00%	0.05%	0.12%
Bacteroidetes	Alistipes.s__Alistipes_indistinctus	0.02%	0.03%	0.13%	0.01%	0.03%	0.16%
Bacteroidetes	Bacteroides.s__Bacteroides_faecis	0.22%	0.10%	0.00%	0.08%	0.05%	0.00%
Actinobacteria	Bifidobacterium.s__Bifidobacterium_longum	0.83%	0.40%	8.91%	0.21%	0.19%	1.13%
Actinobacteria	Eggerthella.s__Eggerthella_lenta	0.19%	1.10%	0.96%	0.10%	0.35%	0.42%
Actinobacteria	Bifidobacterium.s__Bifidobacterium_bifidum	0.47%	0.38%	1.51%	0.21%	0.36%	0.72%
Actinobacteria	Collinsella.s__Collinsella_aerofaciens	1.48%	0.32%	0.77%	0.70%	0.13%	0.30%
Actinobacteria	Bifidobacterium.s__Bifidobacterium_adolescentis	0.99%	0.40%	1.38%	0.33%	0.25%	0.32%
Actinobacteria	Bifidobacterium.s__Bifidobacterium_breve	0.50%	0.00%	0.14%	0.22%	0.00%	0.18%
Actinobacteria	Adlercreutzia.s__Adlercreutzia_equolifaciens	0.01%	0.14%	0.12%	0.01%	0.13%	0.02%
Actinobacteria	Bifidobacterium.s__Bifidobacterium_pseudocatenulatum	0.95%	0.10%	0.16%	0.31%	0.11%	0.19%
Actinobacteria	Bifidobacterium.s__Bifidobacterium_catenulatum	0.03%	0.00%	0.25%	0.02%	0.00%	0.21%
Proteobacteria	Burkholderiales_noname.s__Burkholderiales_bacterium_1_1_47	0.25%	0.13%	0.12%	0.11%	0.12%	0.15%
Proteobacteria	Parasutterella.s__Parasutterella_excrementihominis	0.34%	0.02%	0.22%	0.15%	0.02%	0.17%
Proteobacteria	Cupriavidus.s__Cupriavidus_metallidurans	0.00%	0.03%	0.03%	0.00%	0.04%	0.00%
Proteobacteria	Escherichia.s__Escherichia_coli	0.00%	15.54%	0.34%	0.00%	3.33%	0.11%
Proteobacteria	Bilophila.s__Bilophila_wadsworthia	0.00%	1.18%	0.14%	0.00%	0.10%	0.18%
Proteobacteria	Sutterella.s__Sutterella_wadsworthensis	0.00%	0.17%	1.99%	0.00%	0.16%	0.00%
Verrucomicrobia	Akkermansia.s__Akkermansia_muciniphila	0.21%	0.84%	0.21%	0.09%	0.43%	0.09%

Supplementary Table 3: Microbes shown to play a role in fermentation (following literature search)

All fiber fermenters	Arabinoxyylan	B-fructans	Pectin	B-Glucan
Faecalibacterium.s__Faecalibacterium_prausnitzii	Bifidobacterium.s__Bifidobacterium_longum	Bifidobacterium.s__Bifidobacterium_longum	Bacteroides.s__Bacteroides_fragilis	Bifidobacterium.s__Bifidobacterium_longum
Flavonifractor.s__Flavonifractor_plautii	Bifidobacterium.s__Bifidobacterium_bifidum	Bifidobacterium.s__Bifidobacterium_bifidum	Bacteroides.s__Bacteroides_vulgatus	Bifidobacterium.s__Bifidobacterium_bifidum
Bacteroides.s__Bacteroides_fragilis	Bifidobacterium.s__Bifidobacterium_adolescentis	Bifidobacterium.s__Bifidobacterium_adolescentis	Bacteroides.s__Bacteroides_uniformis	Bifidobacterium.s__Bifidobacterium_adolescentis
Bacteroides.s__Bacteroides_vulgatus	Bifidobacterium.s__Bifidobacterium_pseudocatenulatum	Bifidobacterium.s__Bifidobacterium_pseudocatenulatum	Bacteroides.s__Bacteroides_dorei	Bifidobacterium.s__Bifidobacterium_pseudocatenulatum
Bacteroides.s__Bacteroides_uniformis	Bifidobacterium.s__Bifidobacterium_breve	Bifidobacterium.s__Bifidobacterium_breve	Bacteroides.s__Bacteroides_caccae	Bifidobacterium.s__Bifidobacterium_breve
Bifidobacterium.s__Bifidobacterium_longum	Bifidobacterium.s__Bifidobacterium_catenumulatum	Bifidobacterium.s__Bifidobacterium_catenumulatum	Bacteroides.s__Bacteroides_ovatus	Bifidobacterium.s__Bifidobacterium_catenumulatum
Bacteroides.s__Bacteroides_dorei	Streptococcus.s__Streptococcus_mitis_oralis_pneumoniae	Streptococcus.s__Streptococcus_mitis_oralis_pneumoniae	Bacteroides.s__Bacteroides_coprocola	Bifidobacterium.s__Bifidobacterium_animalis
Blautia.s__Ruminococcus_torques	Peptostreptococcaceae__Clostridium_bartlettii	Peptostreptococcaceae__Clostridium_bartlettii	Bacteroides.s__Bacteroides_thetaiotaomicron	Bifidobacterium.s__Bifidobacterium_pseudolongum
Clostridium.s__Clostridium_asparagiforme	Streptococcus.s__Streptococcus_salivarius	Streptococcus.s__Streptococcus_salivarius	Parabacteroides.s__Parabacteroides_merdae	Ruminococcus.s__Ruminococcus_lactaris
Bacteroides.s__Bacteroides_caccae	Bifidobacterium.s__Bifidobacterium_animalis	Bifidobacterium.s__Bifidobacterium_animalis	Parabacteroides.s__Parabacteroides_disfastonis	Enterococcus.s__Enterococcus_avium
Clostridium.s__Clostridium_symbiosum	Peptostreptococcus.s__Peptostreptococcus_anaerobius	Streptococcus.s__Streptococcus_infantis	Bacteroides.s__Bacteroides_stercoris	Bacteroides.s__Bacteroides_stercoris
Bacteroides.s__Bacteroides_ovatus	Bifidobacterium.s__Bifidobacterium_pseudolongum	Faecalibacterium.s__Faecalibacterium_prausnitzii	Bacteroides.s__Bacteroides_massiliensis	Bacteroides.s__Bacteroides_massiliensis
Blautia.s__Ruminococcus_gnavus	Streptococcus.s__Streptococcus_parasanguinis	Flavonifractor.s__Flavonifractor_plautii	Bacteroidales__Bacteroidales_bacterium_ph8	Bacteroidales__Bacteroidales_bacterium_ph8
Bifidobacterium.s__Bifidobacterium_bifidum	Streptococcus.s__Streptococcus_infantis	Blautia.s__Ruminococcus_torques	Pseudomonas.s__Pseudomonas_stutzeri	
Bacteroides.s__Bacteroides_coprocola		Roseburia.s__Roseburia_inulinivorans	Bacteroides.s__Bacteroides_cellulosilyticus	
Blautia.s__Ruminococcus_obeuum		Ruminococcus.s__Ruminococcus_lactaris	Bacteroides.s__Bacteroides_eggerthii	
Bifidobacterium.s__Bifidobacterium_adolescentis		Pseudomonas.s__Pseudomonas_stutzeri	Bacteroides.s__Bacteroides_xylanisolvens	
Bacteroides.s__Bacteroides_thetaiotaomicron		Roseburia.s__Roseburia_hominis	Bacteroides.s__Bacteroides_plebeius	
Parabacteroides.s__Parabacteroides_merdae		Pseudoflavonifractor.s__Pseudoflavonifractor_capillosus	Bacteroides.s__Bacteroides_faecis	
Parabacteroides.s__Parabacteroides_distansoni		Ruminococcus.s__Ruminococcus_bromii	Parabacteroides.s__Parabacteroides_johnsonii	
Clostridium.s__Clostridium_boleae		Ruminococcus.s__Ruminococcus_callidus	Bacteroides.s__Bacteroides_finegoldii	
Roseburia.s__Roseburia_inulinivorans		Ruminococcaceae__Ruminococcaceae_bacterium_D16	Bacteroides.s__Bacteroides_intestinalis	
Prevotella.s__Prevotella_copri		Roseburia.s__Roseburia_intestinalis	Bacteroides.s__Bacteroides_coprophilus	
Bifidobacterium.s__Bifidobacterium_pseudocatenulatum		Peptostreptococcus.s__Peptostreptococcus_anaerobius	Parabacteroides.s__Parabacteroides_goldsteinii	
Erysipelotrichaceae__Clostridium_gramosum		Bifidobacterium.s__Bifidobacterium_pseudolongum	Bacteroides.s__Bacteroides_salysiae	
Bacteroides.s__Bacteroides_stercoris		Streptococcus.s__Streptococcus_parasanguinis	Bacteroides.s__Bacteroides_nordii	
Clostridium.s__Clostridium_clostridioforme			Prevotella.s__Prevotella_copri	
Ruminococcus.s__Ruminococcus_lactaris			Paraprevotella.s__Paraprevotella_clara	
Burkholderiales__Burkholderiales_bacterium_1_1_47				
Bacteroides.s__Bacteroides_massiliensis				
Bacteroidales__Bacteroidales_bacterium_ph8				
Pseudomonas.s__Pseudomonas_stutzeri				
Roseburia.s__Roseburia_hominis				
Bacteroides.s__Bacteroides_cellulosilyticus				
Bacteroides.s__Bacteroides_eggerthii				
Pseudoflavonifractor.s__Pseudoflavonifractor_capillosus				
Clostridium.s__Clostridium_hathewayi				
Bifidobacterium.s__Bifidobacterium_breve				
Clostridium.s__Clostridium_nexile				
Bacteroides.s__Bacteroides_xylanisolvens				
Ruminococcus.s__Ruminococcus_bromii				
Bacteroides.s__Bacteroides_plebeius				
Bifidobacterium.s__Bifidobacterium_catenumulatum				
Bacteroides.s__Bacteroides_faecis				
Paraprevotella.s__Paraprevotella_clara				
Clostridium.s__Clostridium_leptum				
Parabacteroides.s__Parabacteroides_johnsonii				
Streptococcus.s__Streptococcus_mitis_oralis_pneumoniae				
Peptostreptococcaceae__Clostridium_bartlettii				
Ruminococcus.s__Ruminococcus_callidus				
Ruminococcaceae__Ruminococcaceae_bacterium_D16				
Bacteroides.s__Bacteroides_finegoldii				
Roseburia.s__Roseburia_intestinalis				
Clostridiales__Clostridiales_bacterium_1_7_47FAA				
Bacteroides.s__Bacteroides_intestinalis				
Bacteroides.s__Bacteroides_coprophilus				
Streptococcus.s__Streptococcus_salivarius				
Clostridiaceae__Clostridiaceae_bacterium_JC118				
Parabacteroides.s__Parabacteroides_goldsteinii				
Enterococcus.s__Enterococcus_avium				
Bifidobacterium.s__Bifidobacterium_animalis				
Erysipelotrichaceae__Clostridium_innocuum				
Peptostreptococcus.s__Peptostreptococcus_anaerobius				
Bifidobacterium.s__Bifidobacterium_pseudolongum				
Bacteroides.s__Bacteroides_salysiae				
Streptococcus.s__Streptococcus_parasanguinis				
Streptococcus.s__Streptococcus_infantis				
Bacteroides.s__Bacteroides_nordii				

Supplementary Table 4: Fiber content database for approximate consumption of dietary fibers

Food item	FFQ Baseline Serving Size (g)	Inulin per serving	FOS per serving	B-glucan per serving	pectin per serving	Total fiber/100g	Inulin/100g	FOS/100g	B-glucan/100g	Pectin/100g
Milk	193.3125	0	0	0	0	0.00				
Fruit juice (orange juice)	196.5	0	0	0	0.393	0.20				0.20
Sugar water (Fruitopia)	262.1	0	0	0	0.2621	0.10				0.10
granola bar (chewy 6601 CNF)	24	0	0	0.48	0.36	4.80			2.00	1.50
Yogurt (Activia - promoted by CCFC)	158.4	0	0	0	0	0.00				
High fiber breakfast cereals (All Bran, 100% Bran, Bran Flakes...)	81.875	2.046875	3.029375	3.275	0	15.00	2.50	3.70	4.00	
Other breakfast cereals, hot cereals	268.75	0	0	1.935	0	1.8			0.72	
Commercial sliced white breads	54	0.054	0.054	0.054	0	1.20	0.10	0.10	0.10	
Other white breads (bagels, pita, hamburger/hot dog rolls, tortillas, crusty bread...)	60	0.06	0.06	0.06	0	1.20	0.10	0.10	0.10	
Commercial sliced whole wheat breads, with bran, multigrain, rye bread	66	0.33	1.254	0.1254	0	4.00	0.5	1.90	0.19	
Other whole wheat breads (bagels, pita, hamburger/hot dog rolls, tortillas, crusty bread...)	60	0.3	1.14	0.114	0	4.00	0.5	1.90	0.19	
Peanut Butter	16.35	0	0	0	0.2943	6.00				1.80
Potato	247.125	1.235625	0	0	0.741375	1.40	0.5			0.30
Rice, rice noodles, couscous	145.375	0	0.145375	0.145375	0	0.5-5		0.10	0.10	
Beans, peas, lentils (legumes), hummus, beans with pork	109.05	0	0	0	0.752445	6-8.7				0.69
Tofu and foods with soya or vegetable proteins	157.2	0	0	0	0	2.40				
Sunflower seeds	10.725	0	0	0	0	27.00				
Nuts, peanuts, other seeds (almonds/cashews/pumpkin)	10.725	0	0	0	0.19305	6.00				1.80
Green/yellow beans, green peas, corn	46.2	0	0	0	0.0231	2.00	0.00	0.00	0.00	0.05
Tomatoes	66.5875	0	0.006658	0	0.166468	1.20		0.01		0.25
Broccoli, cauliflower, brussel sprouts, cabbage and coleslaw	32.55	0	0.16275	0	0	3.00		0.5		
Carrots	47.3375	0	0	0	0.3787	3.60	0.00	0.00		0.80
Lettuce	59.2	0	0.1184	0	0	1.20	0.00	0.20		
Green, red, yellow sweet peppers	55.125	0	0	0	0.275625	1.70	0.00	0.00	0.00	0.50
Apple	182	0	0.182	0	1.456	2.4		0.10		0.80
Bananas	118	0.59	0.59	0	1.1092	1.70	0.50	0.50		0.94
Melons (watermelon, cantaloupe, honeydew...)	120.375	0	0.601875	0	0.024075	0.70		0.50		0.02
Oranges, grapefruits, tangerines (citrus fruits)	131	0	0	0	2.2925	2.20		0.00	0.00	1.75
Berries (strawberries, raspberries, blueberries...)	114.1578	0	0.570789	0	1.141578	2.20		0.50		1.00

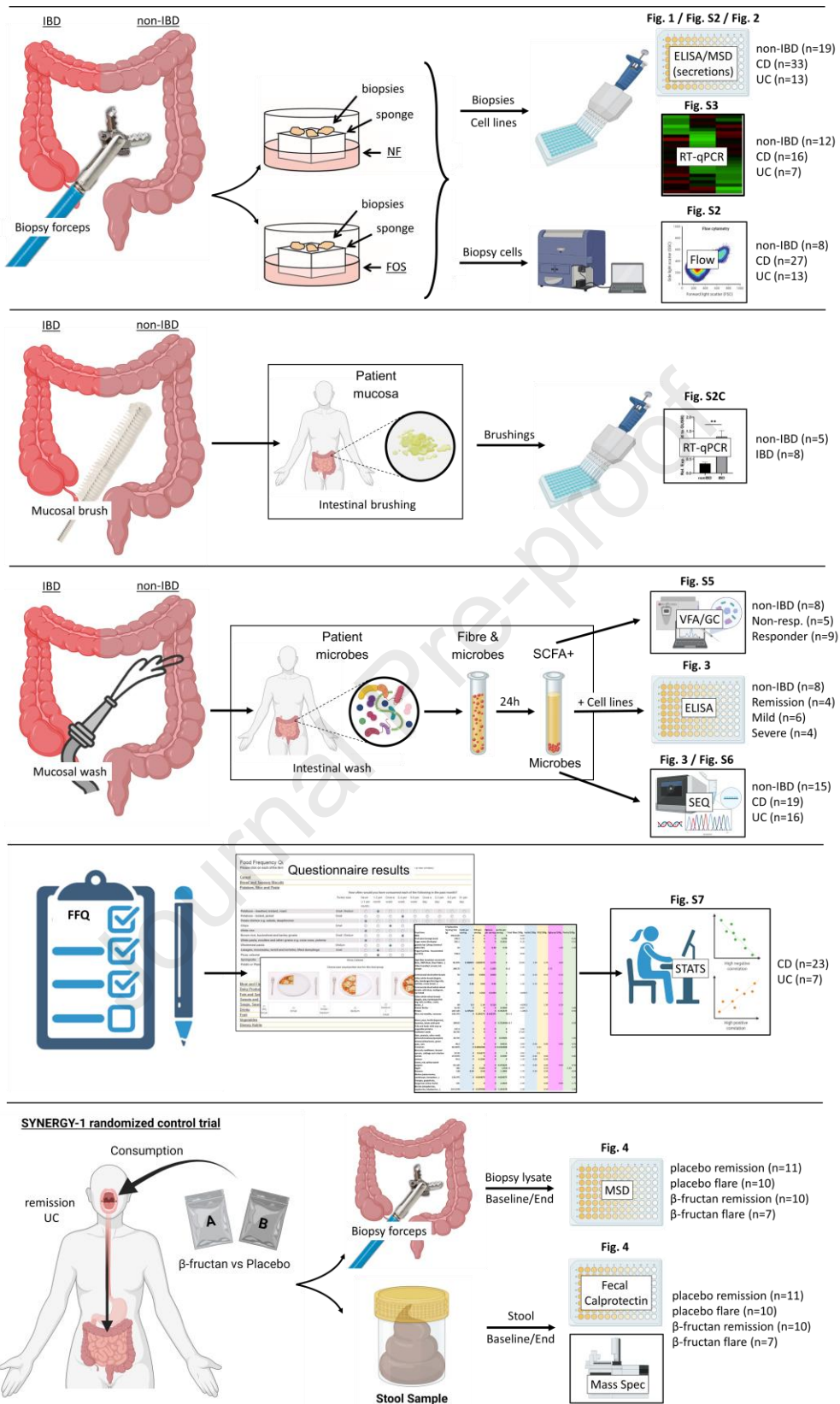
Supplementary Table 5: Patient cohort characteristics

	Non-IBD	CD	UC
Demographics	31	52	29
Male, n (%)	14	32	14
Female, n (%)	17	20	15
Mean age (SD), yrs	12 (4)	13 (3)	14 (3)
Mean disease duration (SD), yrs	n/a	1 (1)	1 (1)
Disease site, n			
Normal	31	17	13
Duodenum		3	
Ileum		1	
Ileocolonic		14	
Terminal ileum		6	1
Cecum		3	2
Pancolonic		11	6
Perianal/rectum		7	2
Descending colon			7
Ascending colon			2
Geboes Histology score			
Remission		16	11
Mild		17	6
Moderate		15	11
Severe		4	1
Therapies at time of collection			
None	31	22	4
Biologics	-	20	9
Infliximab		16	6
Adalimumab		4	2
Vedolizumab			1
Azathioprine		7	5
Methotrexate		12	3
5-Aminosalicylates		2	15
Sulfasalazine			1
Prednisone		1	2

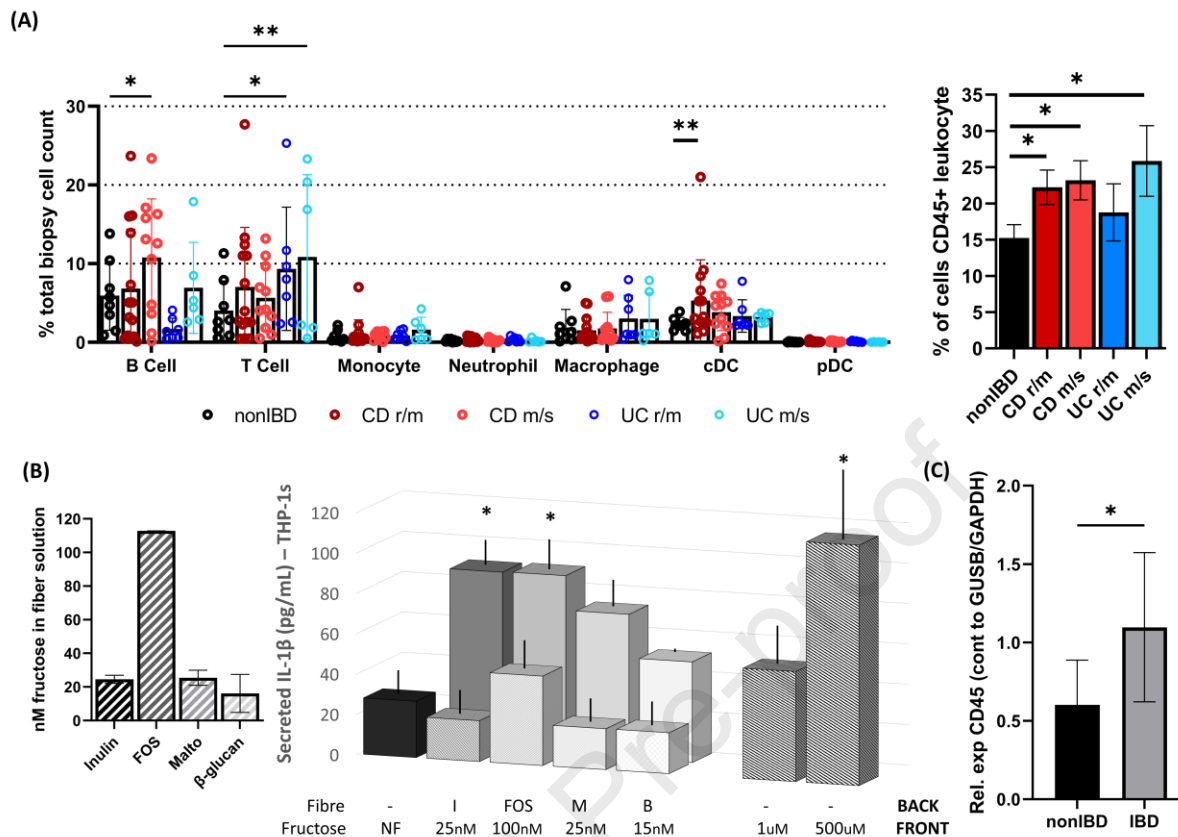
Supplementary Table 6: Primers qRT-PCR

	FWD primer	REV primer
CD45	5'- ACAGCCAGCACCTTTCCTAC	5'- GTGCAGGTAAGGCAGCAGA
GAPDH	5'- CCCACTCCTCCACCTTTGAC	5'- ATGAGGTCCACCACCCTGTT
CX3CL1	5'- GGATGCAGCCTCACAGTCCTTAC	5'- GGCCTCAGGGTCCAAAGACA
GUSB	5'- AAGTCCTTCACCAGCAGCG	5'- CCACGGTGTCAACAAGCAT
NLRP3	QIAGEN Hs_NLRP3_1_SG QuantiTect Primer GeneGlobe Id: QT00029771	
IL-1 β	QIAGEN Hs_IL1B_1_SG QuantiTect Primer GeneGlobe Id: QT00021385	
STAT3	QIAGEN Hs_STAT3_1_SG QuantiTect Primer GeneGlobe Id: QT00068754	
IL23A	QIAGEN Hs_IL23A_1_SG QuantiTect Primer GeneGlobe Id: QT00204078	

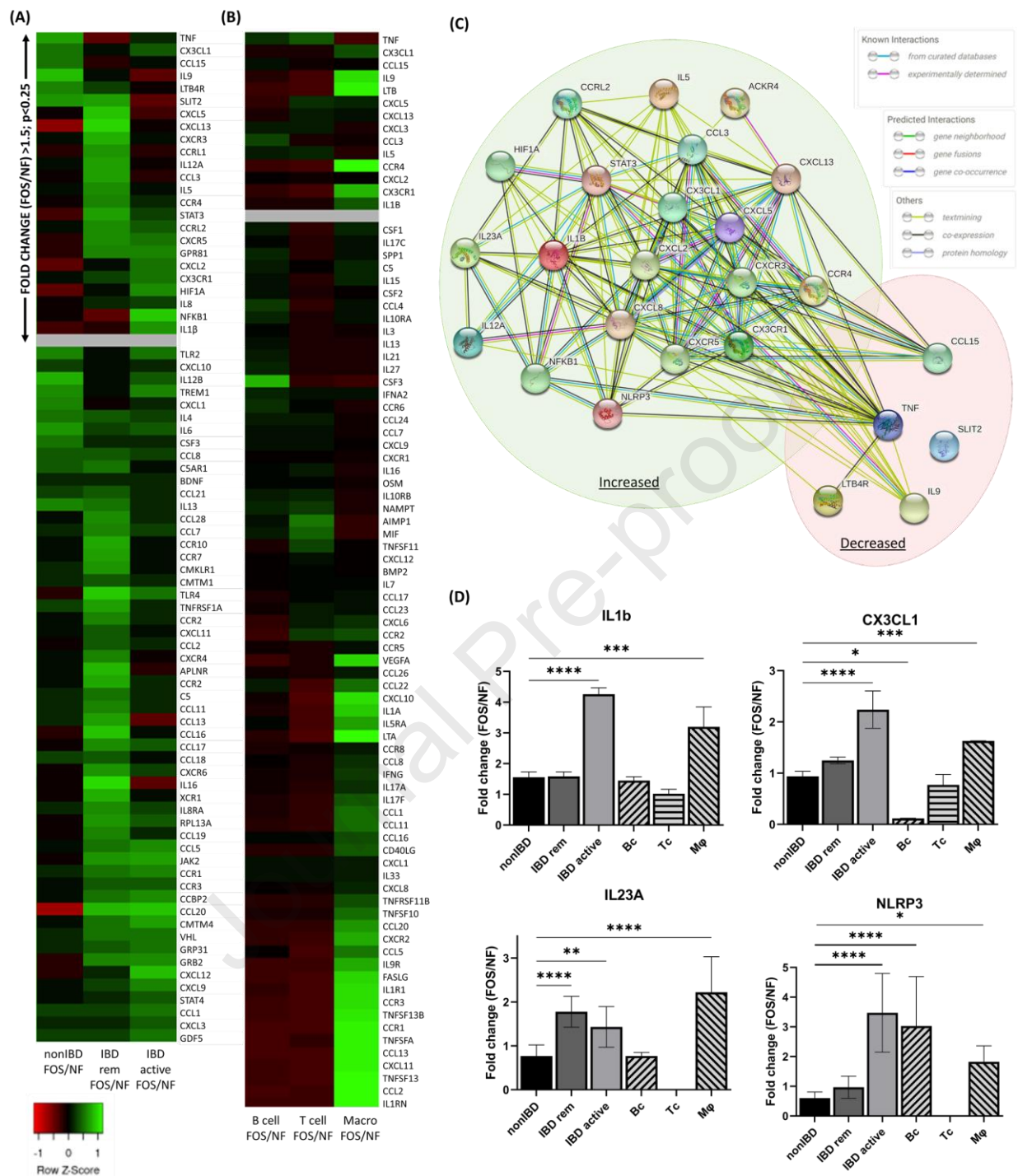
Journal Pre-proof



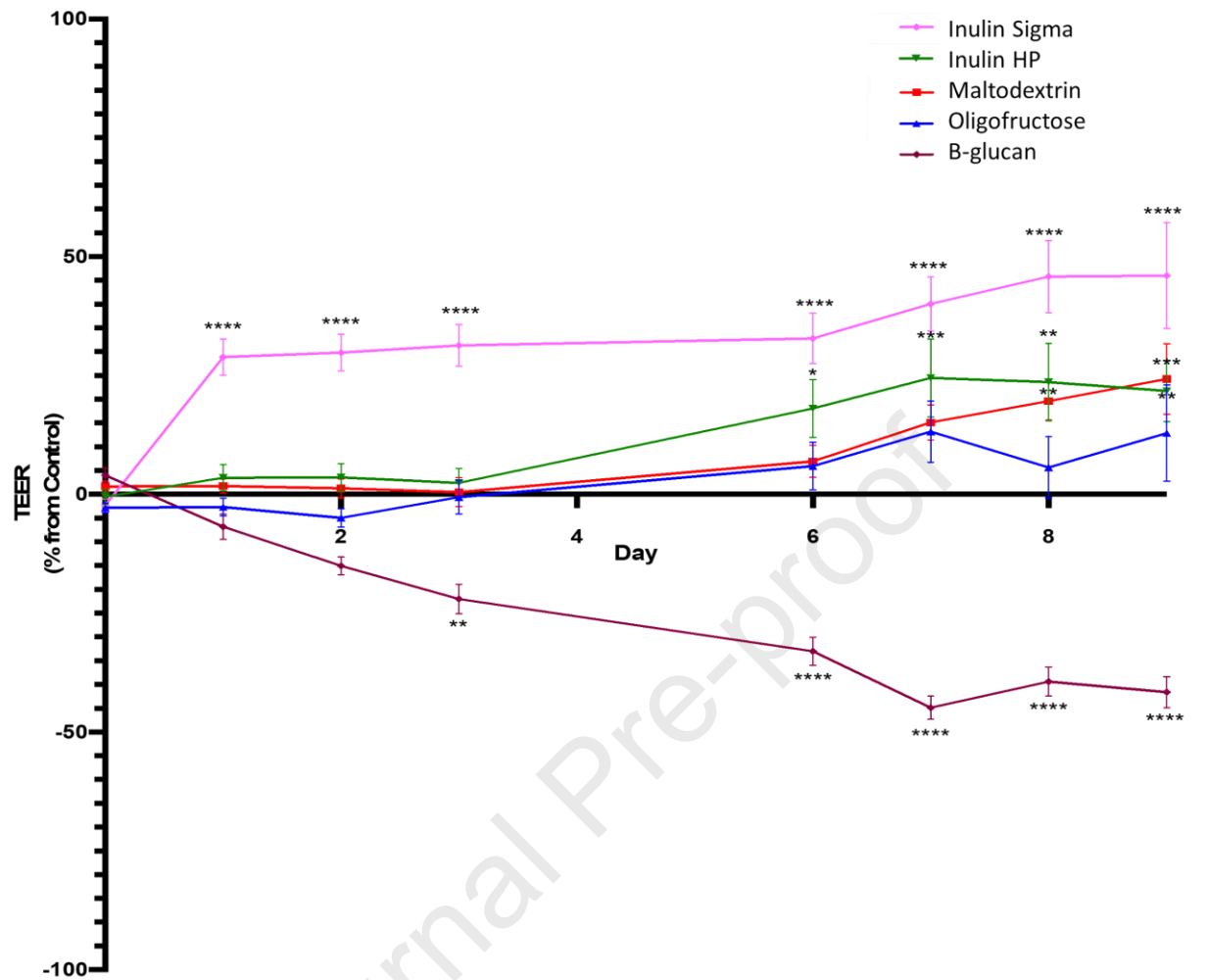
Supplementary Figure 1: Key methods utilized in the collection, preparation, and experimentation of patient materials and cell lines. Figures showing results are referenced for each section; in depth explanation available in the Methods section.



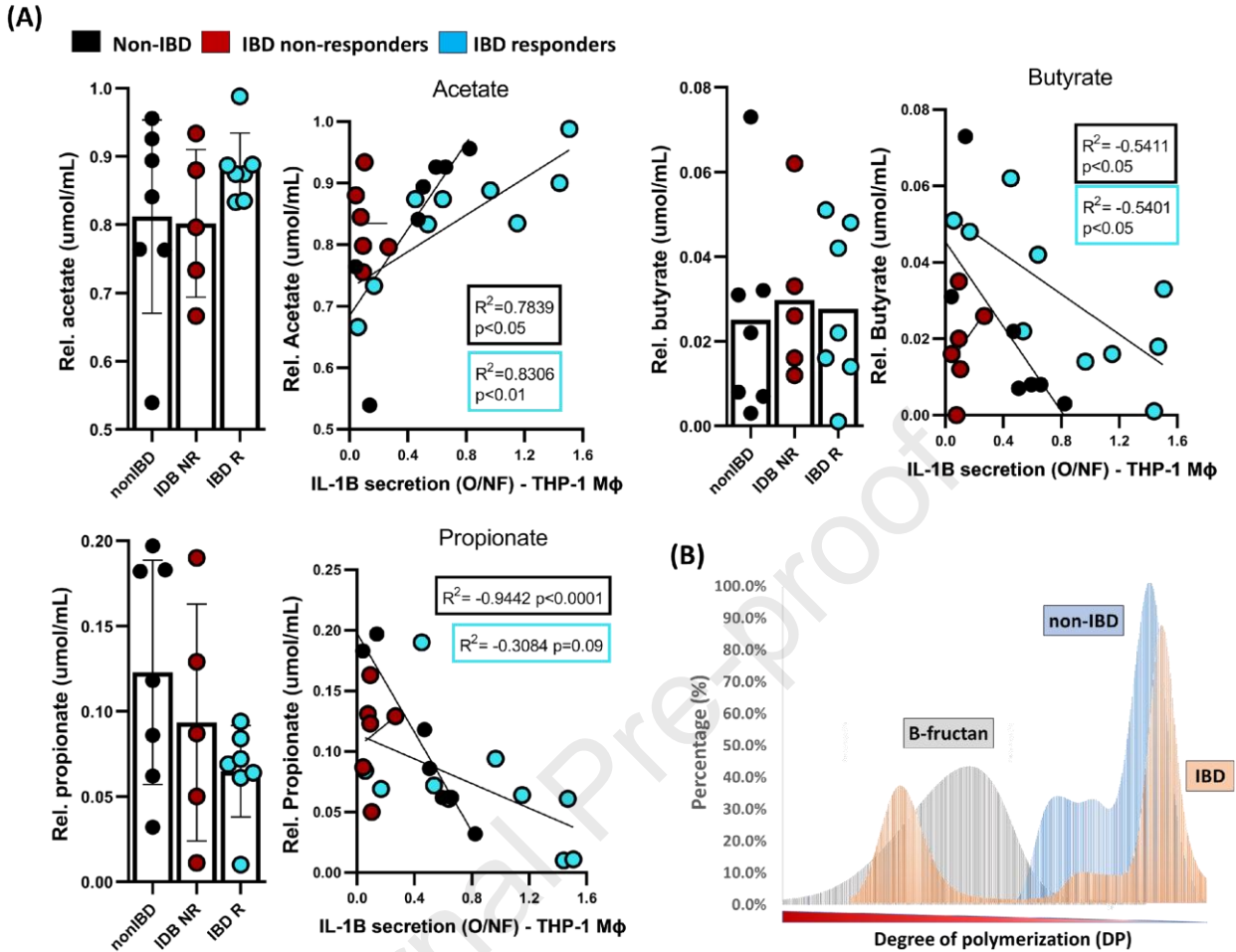
Supplementary Figure 2: Increased immune cells in the mucosa of IBD patients contribute to pro-inflammatory responses driven by interactions of leukocytes with select dietary fibers. (A) Presence of specific immune cell subsets in fresh pediatric non-IBD (n=8), CD (n=27), and UC (n=13) biopsies was measured for B cells, T cells, monocytes, neutrophils, macrophage, classical dendritic cells (cDC), and plasmacytoid dendritic cells (pDC) by multiplex flow cytometry performed on the Attune and total leukocyte number was corrected for CD45. **(B)** The concentration of fructose in inulin, oligofructose, maltodextrin, and β-glucan solutions was determined by fructose assay. THP-1 macrophages were treated with no fiber or fructose (NF), inulin (5 g/L), oligofructose (5 g/L), maltodextrin (5 g/L), β-glucan (1 g/L), or indicated doses of fructose (guided by fructose in Fig S3A) and IL-1β ELISA was on cell secretions. **(C)** Presence of leukocytes at the mucosal surface, confirmed by RTqPCR of CD45 in patient intestinal brushings (n=5 non-IBD, n=8 IBD). *p<0.05, **p<0.01.



Supplementary Figure 3: Identification of pro-inflammatory and barrier integrity changes in response to fiber observed in biopsies from IBD patients and immune cell lines. (A) Pediatric non-IBD (n=3), CD (n=4), and UC (n=4) patient biopsies were cultured *ex vivo* with no fiber (NF) or oligofructose (FOS) and RNA was isolated. Origene CHIP gene array plates identified targets of interest expressed as FOS/NF fold change. (B) Qiagen RT2 profile plates were used to identify changes in cytokines and receptors in cell culture lines *in vitro* treated with FOS or NF control to identify targets of interest in B (n=2), T (n=2), and macrophage (n=2) cells. (C) STRING analysis (ELIXR) outlining connectivity of top genes of interest (FOS/NF fold change > 1.5; p < 0.25), identified by Origene CHIP gene array of pediatric non-IBD (n=3), CD (n=4), and UC (n=4) patient biopsies, cultured *ex vivo* for 24hr. Significant gene targets were validated by (D) RTqPCR of patient biopsy tissues in non-IBD (n=12), IBD remission [CD remission (n=10), UC remission (6), IBD active [CD active (n=3), and UC active (n=4)]. *p < 0.05, **p < 0.01, ***p < 0.001, ****p < 0.0001.

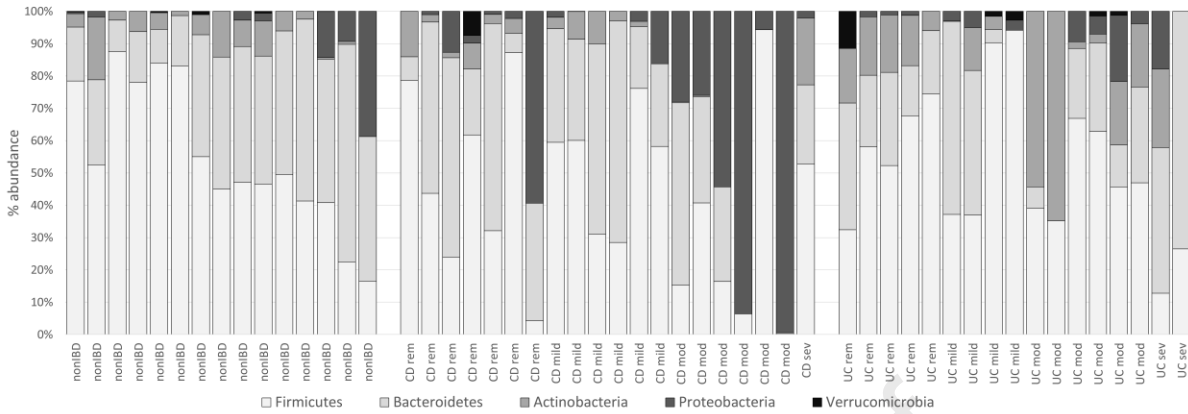


Supplementary Figure 4: Validation of barrier integrity changes in T84 cell culture in response to select dietary fibers of interest. T84 intestinal epithelial cells were grown in Transwell plates and epithelial barrier integrity was examined by Trans Epithelial Electrical Resistance (TEER) assay over time to determine the effect of dietary fibers on gut epithelial cell barrier. ** $p < 0.01$, *** $p < 0.001$, **** $p < 0.0001$.

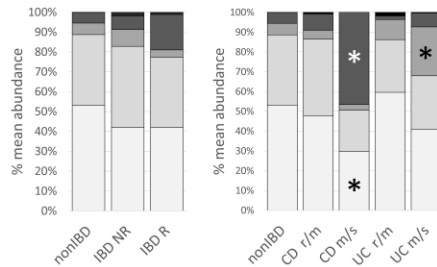


Supplementary Figure 5: By-products of fiber fermentation (SCFA) produced by patient-derived whole microbiome cultures correlated with pro-inflammatory response to fiber in matching biopsy tissues cultured *ex vivo*. (A) Production of volatile fatty acids was measured by VFA/GC in patient whole-intestinal microbe FOS-fermentation supernatants, and correlated with IL-1 β secretion in THP-1 macrophages. Only those of significance (acetate, propionate, and butyrate) are displayed. (B) HPLC was performed to examine the amount of β -fructan remaining in fermentation supernatants following fermentation by active IBD patient or non-IBD participant whole-microbiota cultures.

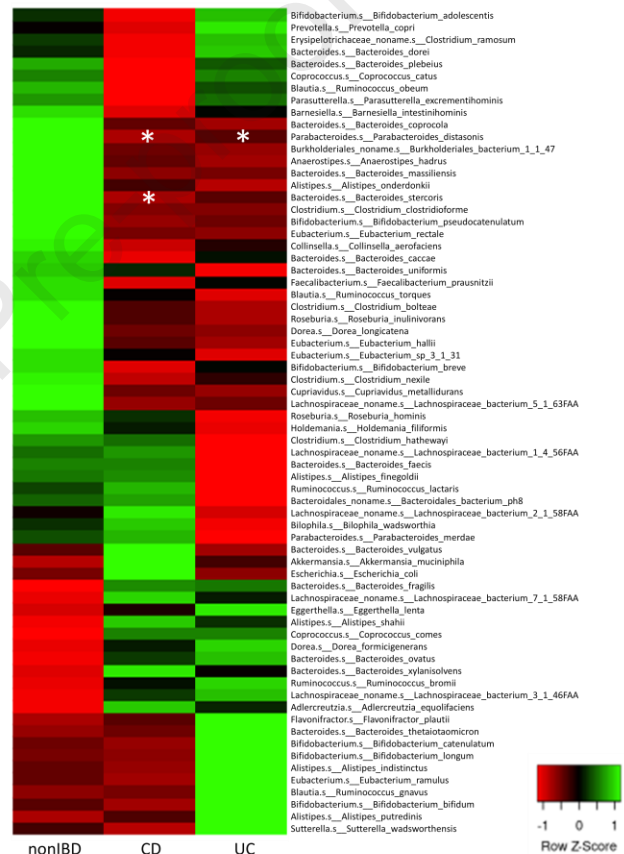
(A)



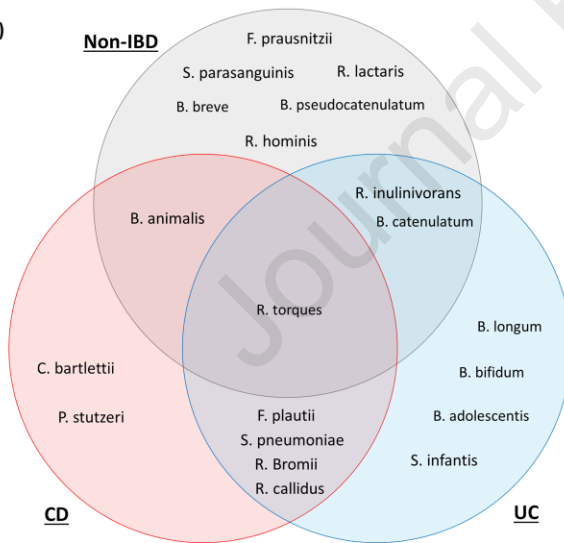
(B)



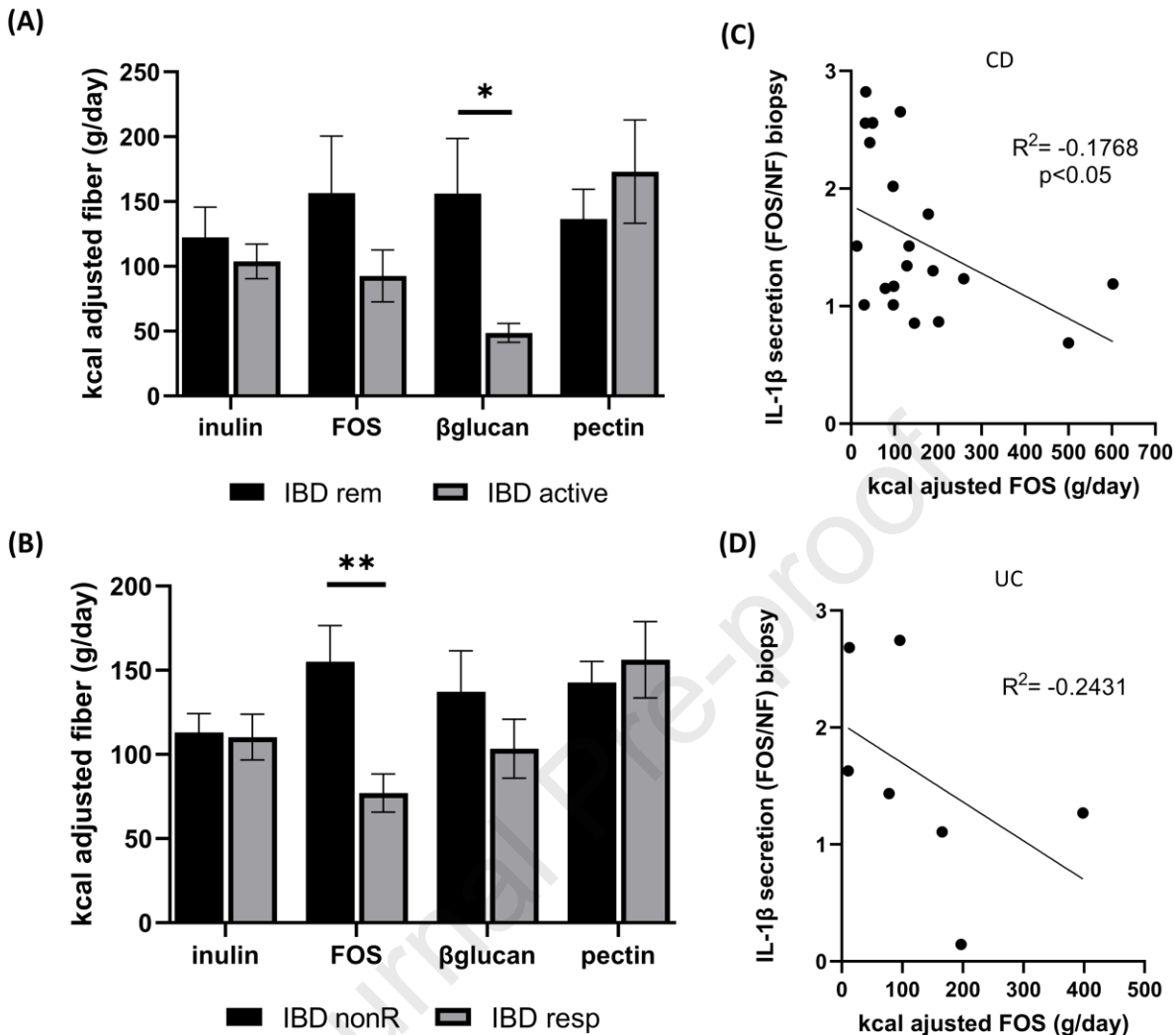
(C)



(D)



Supplementary Figure 6: Microbial function in patient intestinal washes explains the response to dietary fibers in matching patient biopsies. Abundance of select microbial species (determined by shotgun metagenomics sequencing) of pediatric non-IBD ($n=15$), CD ($n=19$), and UC ($n=16$) patient intestinal washes collected during colonoscopy expressed at both the (A) phyla level for individual patients and (B) species level for disease cohorts. (C) Abundance of select microbes involved in fermentation. (D) VENN diagram of select fermentative microbes present in patient intestinal washes.



Supplementary Figure 7: Dietary fiber intake is inversely correlated with *ex vivo* immune response to unfermented fiber. kcal adjusted inulin, oligofructose (FOS), β -glucan, and pectin consumption calculated using FFQs (CD n=23; UC n=7) based on **(A)** disease status (remission n=22; active n=8) and **(B)** IL-1 β response to FOS (non responder n=12; responder [resp] n=18) in biopsies. **(C)** kcal adjusted patient FOS consumption was negatively correlated by Kendall correlative analysis to IL-1 β secretion in response to FOS. **(D)** Consumption of FOS was correlated with abundance of riboflavin synthase in matching patient intestinal washes. * $p < 0.05$, ** $p < 0.01$.